AN EXPERIMENTAL INVESTIGATION ON THE EFFECTS OF BUFFURING REGULATION ON TIME-CRITICAL DELIVERY OF OBJECTS ON A MULTI-CONVEYOR SYSTEM

A Thesis
Presented to
The Academic Faculty

by

Mati C. Chessin

In Partial Fulfillment
of the Requirements for the Degree
Master of Science in Mechanical Engineering in the
School of Mechanical Engineering

Georgia Institute of Technology
May 2007

AN EXPERIMENTAL INVESTIGATION ON THE EFFECTS OF BUFFURING REGULATION ON TIME-CRITICAL DELIVERY OF OBJECTS ON A MULTI-CONVEYOR SYSTEM

Approved by:

Dr. K. M. Lee, Advisor
School of Mechanical Engineering
Georgia Institute of Technology

Dr. A. B. Webster
School of Poultry Sciences
University of Georgia

Dr. W. E. Singhose
School of Mechanical Engineering
Georgia Institute of Technology

Date Approved: 11/27/06

ACKNOWLEDGEMENTS

I wish to thank my advisor Dr. Lee for his endless help and encouragement and his tireless effort to improve the level of my work. I would also like to thank Brianna Walker for her patience and my parents for their concern. Thanks to GTRI for their financial support and to its employees for their emotional support. Much thanks to my committee members Dr. Singhose and Dr. Webster for taking the time to review my thesis and presentation. Additional thanks goes to my former team members Dr. Lan, Ziyen Ng, Qiang Li, Hungsun Son and Shaohui Foong for their help on the Livehang project. Thanks finally to Mark Claffee for showing me it could be done.

TABLE OF CONTENTS

LIST OF TABLES

LIST OF FIGURES

LIST OF SYMBOLS AND ABBREVIATIONS

B_j	The j^{th} object to be processed
BS#0	Beamswitch located at terminal point of 1^{st} conveyor
BS#1	Beamswitch used for position detection
BS#2	Beamswitch used for buffer regulation
$t_{0,j}^{-}$	Time at which object B_j initially triggers BS#1
$t_{0,j}^{+}$	Time at which object B_j clears BS#1
d	Contiguous length of beams that must be blocked to trigger sensor
e_j	Tracking error of object B_j
ε_l	Length measurement error
$\varepsilon_{\Delta S_j}$	Spacing measurement error
$\bar{\varepsilon}_{\Delta t_j}$	Average timing error
ILBTS	Intelligent Live Bird Transfer System
l_j	Actual length of object B_j
$\hat{l}_j$	Measured length of object B_j
l_e	Effective length of object passing through line scanner
L	Length of conveyor
R_a	Radius of curvature of receiving end of conveyor
R_b	Radius of curvature of delivery end of conveyor
S	Mean spacing of objects on the 2nd conveyor
ΔS_j	Actual spacing deviation of object B_j on 2nd conveyor

$\Delta\hat{S}_j$	Measured spacing deviation of object B_j on 2nd conveyor
S_1	Mean spacing of objects on the 1st conveyor
δS_j	Spacing deviation of object B_j on 1st conveyor
S_3	Demanded spacing on 3rd conveyor
$\bar{t}$	
$\bar{t}$	Nominal switch time
$t_{0,j}$	Time at which $x_j = x_0$
$t_{0,j}^-$	Time at which object B_j initially triggers BS#1
$t_{0,j}^+$	Time at which object B_j clears BS#1
$t_{a,i}$	Time at which the object B_i reaches the 2nd conveyor
$t_{f,j}$	Time at which $x_j = x_f$
Δt_j	Timing error of object B_j at time $t = t_{f,j}$
t_s	Time at which velocity switches from v_l to v_h
$\hat{t}_s$	Switch time calculated from improperly measured spacing
T	Demanded cycle time
T_u	Unusable cycle time for buffer regulation
$v_1(t)$	Velocity trajectory of 1st conveyor
$v_3(t)$	Velocity trajectory of 3rd conveyor
$\bar{v}_2$	Average velocity of 2nd conveyor
v_h	High velocity of 2nd conveyor
v_l	Low velocity of 2nd conveyor
x_0	Location of BS#1
x_f	Location of BS#2
$\mathbf{x}$	Direction of motion of all conveyors

y	Global lateral direction across conveyors
z	Global vertical direction
Δz	Vertical drop between conveyors

SUMMARY

This thesis experimentally investigates the effects of buffer regulation on the delivery of randomly spaced objects through a multi-conveyor system according to a demanded throughput and spacing. A regulator is developed and tested in conjunction with on ongoing research project at Georgia Tech investigating the automated transfer of live birds.

In this thesis, an algorithm is proposed to identify and compensate for the spacing deviations of objects entering a system comprised of three serially connected conveyors. The regulator acts to delay the time each object spends on the middle conveyor, eliminating spacing variations by the time objects exit the system. The system is experimentally tested to determine how effectively the algorithm can locate and deliver objects onto specific moving points. The limits of the regulator and the considerations for practical implementation are investigated.

The proposed buffering regulator has immediate applications in the poultry processing industry, wherein live birds must be sorted and hung on a uniform shackle line moving at a constant speed.

CHAPTER 1

INTRODUCTION AND BACKGROUND

1.1. Introduction

In many industries, production lines consist of a series of interconnected systems synchronized to generate a product at a desired line speed. Much of the time, the item being produced is uniform, immobile and easily manipulated. In the poultry processing industry, this is not the case. Some tasks are performed when the birds are alive, so an effective automated machine must be gentle, adaptable to their natural variation in size and weight, and be able to restrict unwanted behavior. At Georgia Tech, a machine has been developed to perform one such task on well spaced birds arriving at a constant rate. The challenge lies in delivering birds to the machine according to this requirement when they arrive with natural variation among their orientation, spacing, size and shape. This thesis investigates the effects of random spacing as well as size/shape variation on the buffering regulator transfer problem.

The remainder of this chapter begins with a review of prior work in systems used in the poultry live transfer task as well as control methods that could be applied to handle such variations. Section 1.3 describes the problem addressed in this thesis and includes a formal problem statement. Section 1.3 highlights the research objectives and the approach taken to solve the problem. Finally, an outline of the thesis is given in Section 1.4.

1.2. Background and Related Work

This thesis addresses a problem commonly encountered in the transfer of natural products for food processing. An example is an ongoing research project at Georgia

Tech entitled "Intelligent Automated Transfer of Live Broilers to Shackle Line" proposed by Lee et al. [1998]. One of the objectives in this project is to invert and load live, randomly-oriented chickens onto a moving shackle line through automation while maintaining industry specifications. This task is currently performed by hand in poultry processing plants, in which roughly one in five workers suffers work-related injuries or illnesses each year, many of which come from the live transfer task [OSHA 2004]. The high injury rate coupled with poor working conditions has created high demand for the automation of this task. The researchers at Georgia Tech have designed and built the Intelligent Live Bird Transfer System (ILBTS) to meet this demand.

Past research works have focused on grasping, shackling and inverting a singulated bird. Lee et al. [1998] investigated experimentally a method of singulating live birds using a set of counter-rotating drums covered with compliant rubber fingers to achieve this task. Lee et al. [2000] continued this work, using FEM analysis to analyze the stresses at the contact areas between a flexible beam and an elliptical object in order to understand the effects of compliant fingers acting on the bird. Summer [2002] developed a kinematic model of the bird's legs in order to design a shackle mechanism. Shumway [2002] analyzed the inversion dynamics of a shackled bird. Yin [2003] investigated the dynamic effects of the bird under the influence of the fingers. Li [2005] investigated the effects of color characterization on the feature detection of live birds using machine vision. Lan [2005] developed several analysis methods to facilitate the design of compliant mechanisms in order to accommodate a limited range of size variations.

In this thesis, the focus is on delivery of birds for subsequent processes such as grasping, shackling and inverting. Birds (with a limited range of size/shape variations) arrive at a processing plant in large containers. The containers are unloaded onto a moving conveyor that will transport the birds into the ILBTS. Once the birds are separated by the counter-rotating drums, they must be properly spaced to undergo further

processing at high speed. It is essential to implement a method to compensate the spacing deviations in real time.

Conveyors are commonly used in transporting poultry meat for processing. Cramer [1976] describes a device that automatically removes the meat from chickens arriving on a shackle line. This machine also relies on the precise timing of birds for transfer and meat removal; however, it does not have to handle spacing uncertainties. The arriving chicken carcasses must already be dressed, eviscerated and hung by their hocks from evenly spaced shackles, facilitating conveyor transfers. Many more machines exist that can handle live birds, such as poultry harvesters. Berry [1994] describes harvesters as feeding birds through a three-rotor pick-up head onto a moving conveyor for collection. While such machines must adapt to a limited range of bird sizes and behaviors, many have less stringent output requirements, often depositing multiple birds into large containers.

The buffering regulator can be treated in several different contexts: regulator design, tracking and repetitive control, discrete time events and switching control. These fields have applications to systems that must compensate for the changing parameters of highly repetitive tasks. When delivering randomly spaced objects of varying size and mass, a static model will not be sufficient to describe the system. Although in the ILBTS, the variations among previous birds do not impact the variations for the current bird, any measurable trend must be taken into account by the controller. One appropriate method for this cause is adaptive control. Adaptive control was developed in the 1950's to aid flight control systems [Dumont and Huzmezan]. As a plane flies, it loses fuel, and thus loses mass. The model must change over time to account for this, creating a time-varying controller. Typical model-reference adaptive systems require using the process inputs and outputs to estimate changes in the model.

Another way to compensate for changing trends is through repetitive control. Formulated by Inoue and Nakano [1981], repetitive control provides a way to

simultaneously track periodic reference signals and reject disturbances for highly repetitive, periodic tasks. The desired input can be learned by feeding the error signal back through the plant over many iterations. If the birds arrive according to a set throughput, they should produce similar periodic inputs. Birds containing unacceptable variation can be rejected or handled by alternate means. As the controller learns more about the incoming objects, zero phase error tracking control (ZPETC) can be used to regulate their spacing. Tomizuka [1987] proposes a feedforward controller based on pole/zero and phase cancellations of a feedback controller. As long as there exist no regulator loop zeros outside or on the unit circle in the z-plane, excellent tracking with smooth velocity occurs. Because ZPETC relies on the pole/zero and phase cancellations, the method is very sensitive to modeling errors and system variations. In conjunction with repetitive or adaptive control, ZPETC could adjust to the changing system to maintain effective delivery.

A different approach often used in manufacturing is modeling a production line as a Discrete Event System (DES). A DES describes a dynamic system that evolves based on physical events occurring abruptly at possibly unknown irregular intervals [Ramadge and Wonham]. The typical system has a discrete state space and piecewise constant state trajectories. The state transitions are called events and generally occur at unpredictable times. The purpose of a DES controller is to drive the system to a desired state by limiting the available events. For the problem at hand, the ILBTS could be modeled as a DES, where the states indicate which conveyor a bird is on and the events are the transfers from one conveyor to another. One reason that DES is often used in manufacturing is that many workcells for discrete production "exhibit the characteristics of a discrete-event system. They are event driven, discrete in time and space, usually asynchronous, and typically nondeterministic" [Lauzon et al.].

An alternative method to model and analyze a DES is by utilizing a Petri net. Petri nets are an extension of graph theory that represents states with nodes and events with

transitions between them. See for example Uzam and Jones [1998], where a specific application of a manufacturing conveyor system is modeled using Petri nets. To reduce the complexity of Petri net systems, it is assumed that the firing of a transition is instantaneous [Peterson]. Because time is continuous, the probability of two instantaneous events occurring simultaneously is zero. Therefore, only one transition can occur at any given time. Another key feature of Petri nets is that there is no need to synchronize the jobs and the processor. As a result, jobs can enter or leave the system independent of current processing. This makes Petri nets well suited to modeling systems of with multiple processes occurring simultaneously, such as the ILBTS. Additionally, there exist methods for robust and adaptive control of discrete event systems [Lin], so, as before, the model can adjust to changing parameters.

Another method to control a delivery system is through switching control, wherein operation of the system is based on switching at discrete-time instances between various low-level continuous-time controllers [Hiyama]. The switch times can be determined in real time based on the performance of system. In the field of optimal control, a classic example is the problem of minimum-time constrained control of a linear system. Porter [1996] showed via genetic methodology that the optimal control law for such a problem evolves towards a "bang-bang" controller, wherein the control signal is set to a maximum value until an optimal time at which it switches to a minimum value. For the delivery of randomly spaced objects, such a controller could calculate the appropriate switch times based on the measured spacing of each object. Ideally, a controller to regulate inputs into the ILBTS should include the best parts of the aforementioned methods.

1.3. Problem Description

This thesis discusses the spacing of objects traveling on a multi-conveyor system. The system consists of multiple conveyors connected serially. For each conveyor in the

system, there is a desired spacing between objects, which vary in size and orientation. In this thesis, the center-to-center distance along the direction of motion, shown as Δx in Figure 1-1, will be used to describe the spacing of interest, for which there exists some desired, nominal value. The spacing deviation is defined as the discrepancy between the actual and nominal spacing.

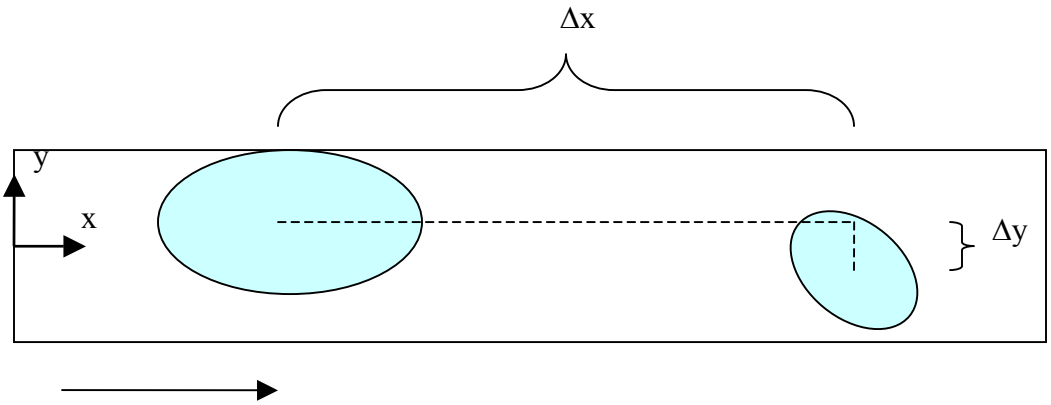

Figure 1-1: Spacing Deviations

Although the techniques developed in this thesis have an immediate application to the live-bird transfer task, the buffering regulator will be developed for the processing of any generic object. It is expected that the objects contain natural variations, as delivery of such objects is the focus of this thesis, but it is desired that they all be similar in size and shape. The objectives for this thesis are as follows:

1. Develop a buffering regulator for a three conveyor system based on the spacing deviations of objects such that the objects exit the system loaded onto equally spaced points at a specified throughput.
2. Simulate, implement and evaluate the regulator for controlling the three-conveyor system.
3. Investigate the effects of buffer regulation on the delivery of known objects with respect to their initial spacing and shape.

The following assumptions are made throughout this thesis: The conveyors have horizontal operating surfaces, which travel only along the **x** direction. Objects arrive and

leave the conveyors according to a given throughput. Also given are the velocity trajectories of the first and third conveyors. Sensors are used at known positions along the system to discretely locate objects, which are spaced such that sensors can distinguish one from the next. It is essential that objects do not move relative to the conveyor surface except during the transfer between conveyors, because the controller cannot directly measure the object location. It can only do so indirectly while the sensors are triggered. If the object moves at any point after triggering a sensor, it will create a measurement error.

1.4. Thesis Outline

The remainder of this thesis is organized as follows. Chapter 2 contains the basis of the buffering regulator. It also provides an overview, highlighting a typical path an object would take through the system, along with a discussion of the relevant parameters and a derivation of the calculations necessary for implementation and evaluation.

Chapter 3 focuses on the experimental setup in order to determine the nominal operating conditions for the system. It presents an algorithm by which the buffering regulator can be implemented. The chapter ends with a simulation investigating the performance of the algorithm with respect to various initial conditions.

Chapter 4 experimentally investigates the effects of buffer regulation. It contains the description and results of four experiments that test the performance of the algorithm for a variety of initial conditions and objects. Components of the algorithm are tested systematically to identify its limitations and to quantify its efficacy.

Chapter 5 considers issues regarding practical implementation of the algorithm, particularly for a system that processes live objects. Through experimentation, it investigates the effects of additional variability in spacing and shape on the performance of the algorithm. Chapter 6 summarizes the key contribution of this thesis and suggests areas of future work.

CHAPTER 2

BUFFER REGULATION

2.1. Introduction

This chapter focuses on developing a buffering regulator for the delivery of randomly spaced objects according to a specified throughput and spacing. The calculations necessary to implement the method are derived along with a means to evaluate its performance and limitations.

2.2. Problem Description and Control Objectives

Without loss of generality, we consider here three serially connected conveyors taken from a typical production line as shown in Figure 2-1. Incoming objects on the 1st conveyor are randomly spaced from a normal distribution of mean S_1 and standard deviation σ_1. They are delivered one at a time to the 2nd conveyor (for example, by means of a singulator), which in turn delivers them to the 3rd conveyor, where the objects must be evenly spaced for subsequent processing. The effects of singulators (or other mechanisms) can be modeled as time delays, τ_1 and τ_2, necessary to transfer an object from the 1st conveyor to the 2nd and from the 2nd conveyor to the 3rd, respectively. The delay τ_2 is included for the completeness of the formulation but its effects will not be experimentally investigated in this thesis.

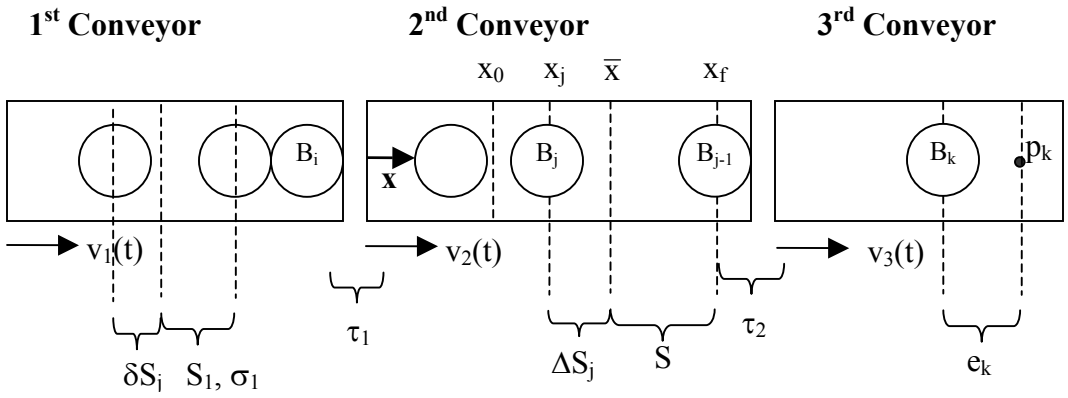

Figure 2-1: System Parameters

As shown in Figure 2-1, the global coordinate frame is assigned at the arrival point on the 2nd conveyor. The objects reach a steady state on this conveyor before x_0. When an object reaches x_f, it will leave the 2nd conveyor and be loaded onto the 3rd conveyor at a specified throughput and spacing. In Figure 2-1, object B_j, whose center is located at x_j, represents the j^{th} object being processed; S is the nominal spacing on the 2nd conveyor; and ΔS_j is the corresponding spacing deviation (or the amount that the distance between x_j and x_{j-1} differs from S). On the 1st conveyor, the corresponding spacing deviation of object B_j is δS_j.

The control objective is to deliver the objects onto equally spaced points on the 3rd conveyor to meet the demanded throughput. In other words, the k^{th} object should arrive on the 3rd conveyor at a specified moving point, p_k, where e_k is the tracking error, i.e., the distance between x_k and p_k. The times at which object B_j reaches x_0 and x_f are $t_{0,j}$ and $t_{f,j}$ respectively, where the first subscript "0" or "f" denotes the location and the second subscript "j" denotes the object number. The relationship between these variables can be summarized as follows:

At $t = t_{f,j-1,}$ $$x_{j-1} = x_f \quad \textbf{(2-1)}$$

$$\Delta S_j = x_f - x_j - S \quad \textbf{(2-2)}$$

At $t = t_{f,j-1} + \tau_2$: $$e_{j-1} = x_{j-1} - p_{j-1} \quad \textbf{(2-3)}$$

The 1st and 3rd conveyors operate at given velocity trajectories, $v_1(t)$ and $v_3(t)$, respectively; and the speed of the 2nd conveyor, $v_2(t)$, adjusts based on the spacing deviation of the objects it transports. Because the 2nd conveyor's motion will equally affect the location of all objects upon it, the spacing between any two objects can only be changed when they lie on neighboring conveyors. Thus, the 2nd conveyor is used for buffer regulation, in that once B_{j-1} reaches x_f, B_j should be kept on the conveyor for only as long as is dictated by the throughput. Any deviation from this time will result in objects on the 3rd conveyor without the proper spacing.

2.3. Measurable and Control Variables

The tracking control is performed by manipulating the 2nd conveyor through $v_2(t)$, which is monitored through an incremental encoder mounted on the driven shaft. In order to accurately deliver objects, two additional proximity sensors are rigidly mounted on the 2nd conveyor, the 1st (hereafter referred to as BS#1) located at $x_{0,}$ and the 2nd (BS#2) at x_f as indicated in Figure 2-1.

BS#1 detects the object B_j as it crosses $x_j = x_0$ at time $t_{0,j}$. Since x_j is known at this time, $S+\Delta S_j$ can be determined from the distance traveled by the conveyor since object B_{j-1} previously triggered BS #1 at time $t_{0,j-1}$. BS#2 detects B_j at $x_j = x_f$ at time $t_{f,j-1}$ before it transfers onto the 3rd conveyor. When B_{j-1} triggers BS#2, the 2nd conveyor completes its transfer process and must switch to handling object B_j. The relationship between the conveyor motion, the object locations and the sensor information is illustrated in Figure 2-2 and given mathematically as follows:

At $t = t_{0,j-1}$,
$$x_{j-1} = x_0 \tag{2-4}$$

At $t = t_{f,j-1}$,
$$x_{j-1} = x_0 + \int_{t_{0,j-1}}^{t_{f,j-1}} v_2(t)dt = x_f \tag{2-5}$$

$$x_j = x_0 + \int_{t_{0,j}}^{t_{f,j-1}} v_2(t)dt > x_0 \tag{2-6}$$

In Equations (2-4), (2-5) and (2-6), x_0 and x_f are given, $v_2(t)$ is measured by the encoder, $t_{0,j}$ and $t_{0,j-1}$ are measured by BS#1 and $t_{f,j-1}$ is measured by BS#2. These sensors together provide the measurements to the existing system's controller. As shown in Figure 2-2, the position of each object is only known once it crosses x_0. For the time between $t_{0,j}$ and $t_{f,j-1}$, the spacing between the objects can not change, resulting in parallel trajectories. More information on the operation of the sensors will be discussed in Section 2.5.

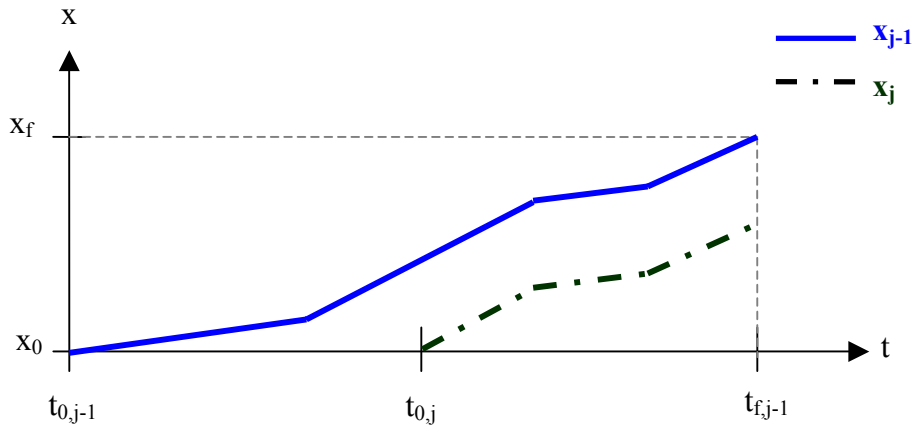

Figure 2-2: Position Trajectories for B_j and B_{j-1}

As discussed in Section 2.2, the spacing deviations of the objects are compensated by $v_2(t)$. However, the existing system is configured to produce only two commanded speeds, a low speed v_l and a high speed v_h. To appropriately regulate the tracking error of delivered objects, a switching controller is designed to manipulate the time t_s at which the 2nd conveyor switches from one speed step to the other. By changing the speed based on the spacing deviation, the controller creates a buffer for the current object. Figure 2-3 and Figure 2-4 show respectively the displacement and velocity of the j^{th} object and velocity of a nominal case, in which there is no spacing deviation for object B_j. The velocity changes at an operating point $\bar{t}$, and object B_j reaches x_f according to the throughput. This thesis experimentally investigates the effects such a controller has on the tracking error of objects exiting the system.

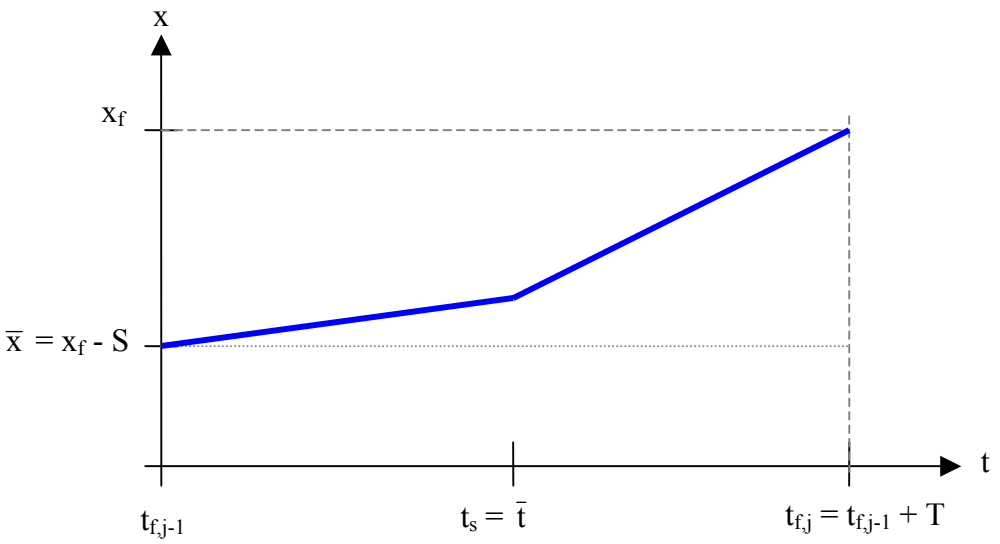

Figure 2-3: Switching Control for Nominal Position

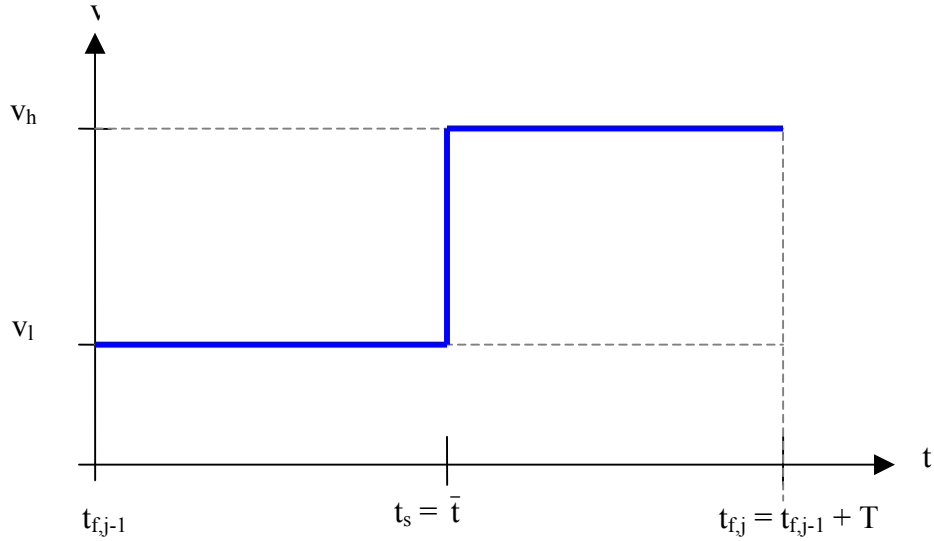

Figure 2-4: Switching Control for Nominal Velocity

2.4. Buffered Velocity Trajectory

Handling multiple objects with respect to a throughput is a cyclic operation of period T, which is a nominal cycle time given by the demanded time between objects exiting the system. The time $t_{f,j}$ at which object B_j reaches x_f should be T seconds after B_{j-1} crosses BS #2. The timing error, Δt_j, is defined as the difference between the actual

delivery time and this expected value, as shown in Equation (2-7). Improper timing could occur due to a measurement or execution error.

$$\Delta t_j = t_{f,j} - (t_{f,j-1} + T) \tag{2-7}$$

Based on the nominal spacing S, the average velocity $\bar{v}_2$ can be calculated from Equation (2-8),

$$\bar{v}_2 = \frac{S}{T} = \frac{v_l + v_h}{2} \tag{2-8}$$

where the two fixed speeds, v_l and v_h, are chosen such that $\bar{v}_2$ is halfway between them. Since the conveyor can only move at one of these two speeds, it will never operate at the average velocity.

The buffering is regulated by beginning each cycle at v_l then switching to v_h at a calculated switch time, t_s. The corresponding nominal switch time $t_s = \bar{t}$, which lies at the midpoint of the cycle, is given by Equation (2-9).

$$\bar{t} = t_{f,j-1} + \frac{T}{2} \tag{2-9}$$

During a typical operation, object B_j, will contain some spacing deviation ΔS_j. If the current object B_j is too close to the previous object B_{j-1}, the conveyor must slow down to increase the spacing. This is accomplished by moving t_s further in the cycle, implying that object B_j will spend longer at a slow speed. If instead the objects B_j and B_{j-1} are too far apart, the conveyor should speed up by decreasing t_s. For an ideal system, t_s is derived as follows:

$$S + \Delta Sj = v_l\left(t_s - t_{f,j-1}\right) + v_h\left(t_{f,j-1} + T - t_s\right)$$

$$\bar{v}_2 T + \Delta Sj = \left(v_h - v_l\right)\left(t_{f,j-1} - t_s\right) + v_h T$$

$$\frac{T\left(\bar{v}_2 - v_h\right) + \Delta S_j}{v_h - v_l} = \left(t_{f,j-1} - t_s\right)$$

$$t_s = t_{f,j-1} + \frac{T(v_h - \bar{v}_2) - \Delta S_j}{v_h - v_l} \quad \begin{cases} < \bar{t} & \text{if } \Delta S_j > 0 \\ = \bar{t} & \Delta S_j = 0 \\ > \bar{t} & \Delta S_j < 0 \end{cases} \qquad \textbf{(2-10)}$$

Figure 2-5 and Figure 2-6 illustrate three cases ($\Delta S_j > 0$, $\Delta S_j < 0$, $\Delta S_j = 0$), in which the operation of the system differs from the nominal trajectories shown in Figure 2-3 and Figure 2-4.

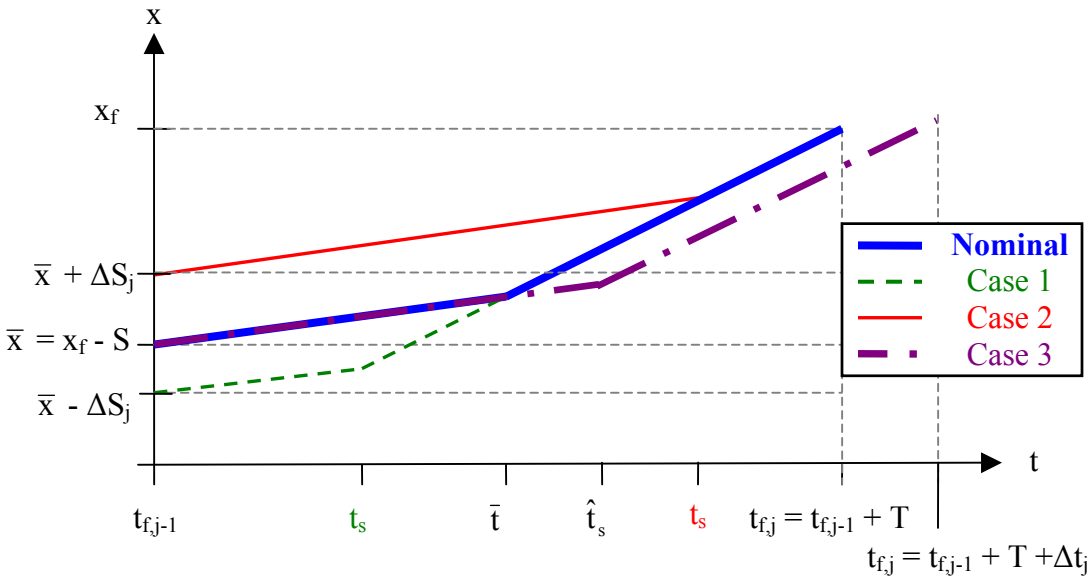

Figure 2-5: Theoretical Effect of Buffering on Position

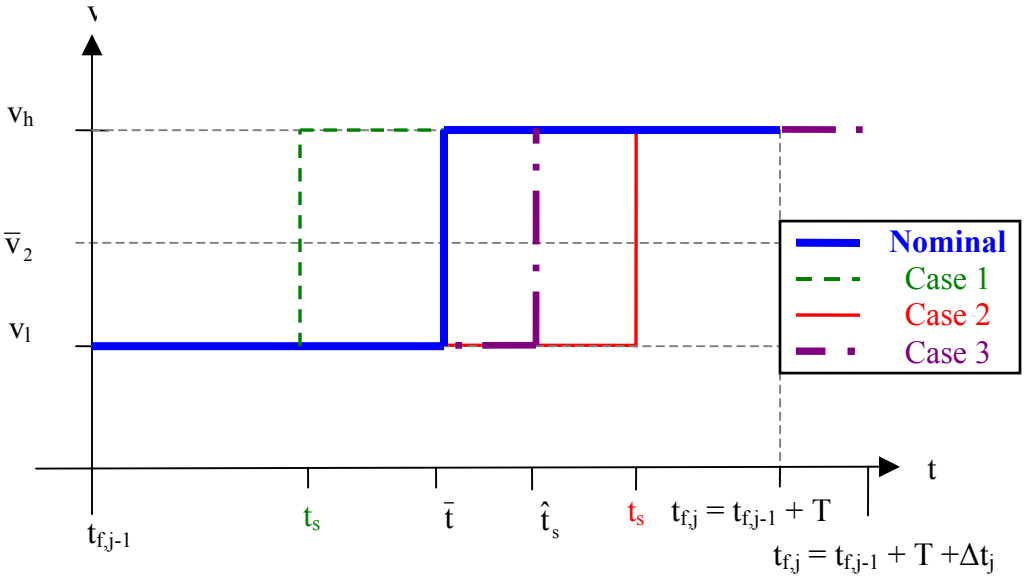

Figure 2-6: Theoretical Effect of Buffering on Velocity

To properly deliver object B_j with a positive deviation as illustrated in Figure 2-1, $t_s < \bar{t}$, labeled as Case #1. The two paths unite after $t = \bar{t}$, meaning that ΔS_j has been eliminated. On the other hand, Case #2 shows the trajectory when object B_j is too close, for which the paths unite at $t = t_s > \bar{t}$. Case #3 shows an example path of an object that is not properly delivered. This could happen, for example, due to a measurement error. The switch time is calculated later than desired, at $t = \hat{t}_s > t_s$. Even though object B_j began the cycle with no spacing deviation, it reaches x_f later than desired, with a positive timing error Δt_j. In order to adequately meet the demanded throughput and spacing, timing errors must be minimized.

Spacing Bounds

Another potential cause of improper delivery is the initial spacing of objects. The assumption that v_l is constant imposes certain bounds for the buffer regulation to work. These bounds are listed as follows:

1) $t_s < t_{f,j-1} + T$ **(2-11)**

2) $t_s > t_{f,j-1}$ **(2-12)**

If Equation (2-11) is violated the conveyor must operate at v_l for longer than T seconds and at v_h for a negative time in order to properly deliver the object. This occurs when B_j is too close to B_{j-1}. The lower spacing limit can be determined by substituting t_s from Equation (2-10) into Equation (2-11) as follows:

$$t_{f,j-1} + \frac{T(v_h - \bar{v}_2) - \Delta S_j}{v_h - v_l} < t_{f,j-1} + T$$

$$Tv_h - (\Delta S_j + S) < T(v_h - v_l)$$

$$\Delta S_j + S > Tv_l$$

$$\frac{\Delta S_j}{S} > \frac{v_l}{\bar{v}_2} - 1 \qquad \textbf{(2-13)}$$

Likewise, if Equation (2-12) is violated, the conveyor must operate at v_h for longer than T seconds and at v_l for a negative time. This occurs when object B_j is too far from object B_{j-1}. The upper spacing limit can be determined by substituting t_s from Equation (2-10) into Equation (2-12) as follows:

$$t_{f,j-1} + \frac{T(v_h - \bar{v}_2) - \Delta S_j}{v_h - v_l} > t_{f,j-1}$$

$$Tv_h - (\Delta S_j + S) > 0$$

$$\Delta S_j + S < Tv_h$$

$$\frac{\Delta S_j}{S} < \frac{v_h}{\bar{v}_2} - 1 \qquad \textbf{(2-14)}$$

The above spacing bounds hold only for the theoretical trajectory shown in Figure 2-6, where the velocity can change instantaneously. In practice, the acceptable range of spacing deviations is further reduced due to the conveyor dynamics, the controller's processing time, the time required to operate the sensors and the time delay required for an object to change conveyors. Taken together, T_u is the total amount of unusable cycle time during which t_s can not occur, as calculated in Equation (2-15),

$$T_u = 2\,T_r + T_{pd} + T_{br} + nT_{bs} + \tau_2 \qquad \textbf{(2-15)}$$

where T_r is the characteristic time of the 2nd conveyor; T_{pd} is the processing time required to detect the position and spacing of an object; T_{br} is the processing time required to implement the buffering regulation; T_{bs} is the processing time to operate the sensors; n is the number of sensor scans required each cycle. These will be discussed in more detail below.

Conveyor Dynamics

Due to the conveyor acceleration, it will take a finite amount of time to change between the two buffering speeds. As mentioned, T_r is characteristic time of the 2nd conveyor, defined as the time needed for the speed change, as shown in Figure 2-8. If the conveyor accelerates and decelerates at the same rate, then the conveyor must complete a full velocity change from v_h to v_l and a second back to v_h in order to travel the required distance each cycle. If one of these changes is cut short, the object can not be properly delivered. Therefore, the usable cycle time in which the switch can occur is reduced by twice the characteristic time. To illustrate this effect, consider object B_j being processed, as shown in Figure 2-7 and Figure 2-8.

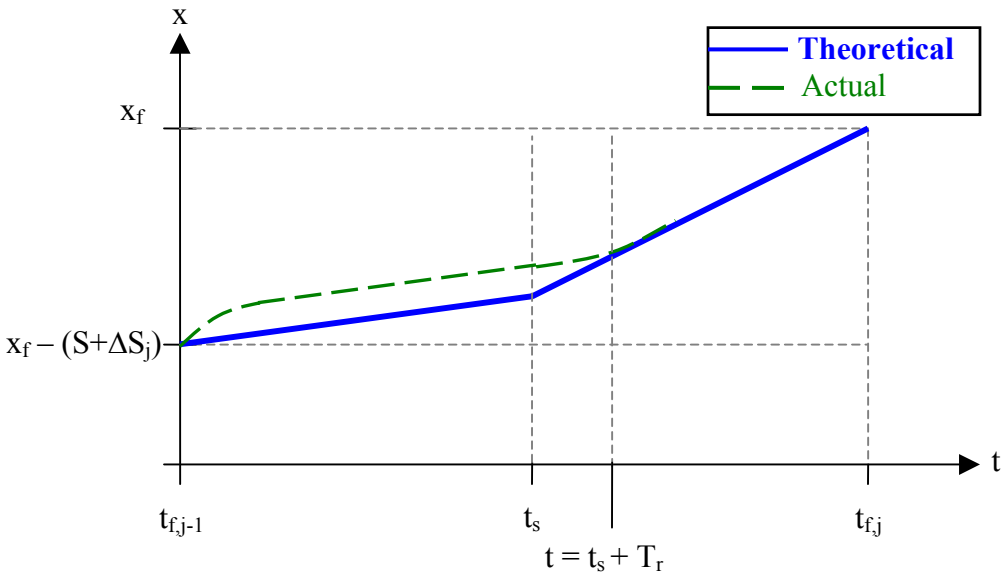

Figure 2-7: Effect of Buffering on Position

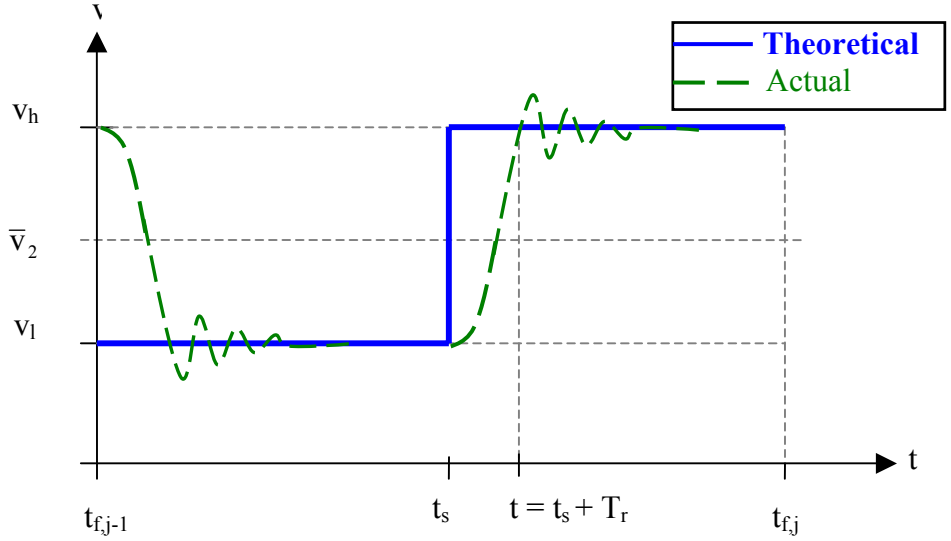

Figure 2-8: Effect of Buffering on Velocity

As object B_{j-1} triggers BS #2, the 2nd conveyor should be running at v_h from the end of the previous cycle. Just as object B_{j-1} leaves the conveyor, the speed changes to v_l. Since the conveyor requires T_r seconds to change speeds, object B_j initially travels further than desired, as shown by the distance between the trajectories in Figure 2-7. At time t_s, the conveyor will take another T_r seconds to reach v_h. During this time, object B_j should lag relative to the theoretical case by the same amount that it lead initially. At $t = t_s + T_r$, these discrepancies should cancel.

Processing Times

The processor requires a finite amount of time to perform the calculations used to locate the objects and determine the switch time. On average, one object should pass through each sensor per cycle. Therefore, the time required to perform one position calculation, T_{pd}, and the time required to perform one t_s calculation and implementation, T_{br}, must also be subtracted from the cycle time when determining the spacing bounds. Another element that affects the usable cycle time is the time required to do a sensor scan, T_{bs}. The sensors continuously scan to see if an object is triggering it. The sensors must scan a minimum of n times each cycle to gather the necessary data. The extra scans

that occur do not affect the usable cycle time because the controller waits for a change in signal, rather than processing the output of every scan. Finally, the mechanism by which the object transfers to the 3rd conveyor requires that the object be moving at v_h. While this transfer occurs, the conveyor speed should not change.

Based on the above reasoning, the switch time t_s must occur within the cycle's usable time. For object B_j, this time is calculated in (2-16). To meet this requirement, the allowable spacing bounds can be calculated using Equation (2-17), which is derived using the same method as for Equations (2-11) and (2-12).

$$\frac{T - T_u}{2T} < \frac{t_s - t_{f,j-1}}{T} < + \frac{3T - T_u}{2T} \quad \textbf{(2-16)}$$

$$\left| \frac{\Delta S_j}{S} \right| < \frac{v_h - v_l}{2} \left(\frac{T - T_u}{S} \right) \quad \textbf{(2-17)}$$

Arrival Stability

In order to study the effects of buffer regulation on object delivery, an important measure used is the change in spacing deviations of objects over time. If the spacing deviation grows over time, the system becomes unstable. For this reason, we formulate a basis to analyze the stability. We consider here object B_i arriving on the 2nd conveyor during processing of object B_j as shown in Figure 2-9 a sensor (BS#0) is located at $x = x_a < 0$. There can be any number of objects in between B_{i-1} and B_j.

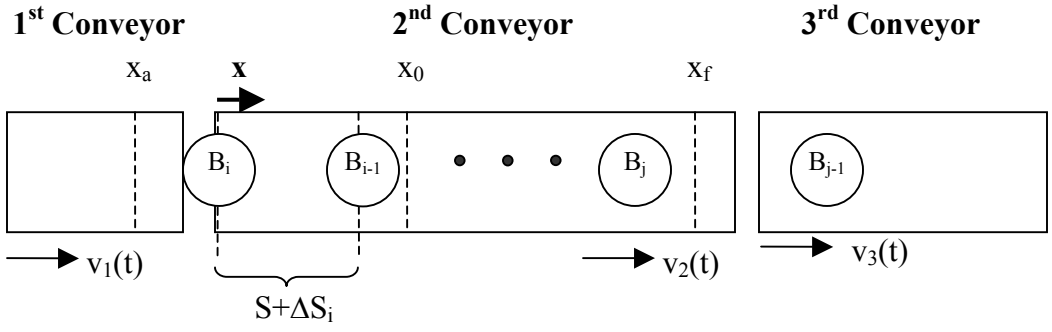

Figure 2-9: Schematic of Arriving Object

Object B_i triggers BS#0 at time $t_{a,i}$, and transfers onto the 2nd conveyor over the fixed time τ_1. The time $t_{a,i}$ is a function of the initial location of B_i on the 1st conveyor.

At $t = t_{a,i} + \tau_1$,

$$x_i = 0 \quad \textbf{(2-18)}$$

$$x_0 < x_j < x_f \quad \textbf{(2-19)}$$

$$x_{j-1} > x_f \quad \textbf{(2-20)}$$

The previous object B_{i-1} arrives on the 2nd conveyor at time $t = t_{a,i-1}$. On average, the object B_i should arrive T seconds later, though due to variations in initial spacing, it is hardly expected. The spacing deviation of object B_i will be dictated by $v_2(t)$ over this elapsed time, as shown in Equation (2-21).

$$\Delta S_i = \int_{t_{a,i-1}+\tau_1}^{t_{a,i}+\tau_1} v_2(t)dt - S \quad \textbf{(2-21)}$$

If the objects B_i and B_{i-1} arrive on the 2nd conveyor at the exact times objects B_j and B_{j-1} depart respectively, Equation (2-21) can be reduced to Equation (2-22).

$$\Delta S_i = \int_{t_{f,j-1}}^{t_{f,j}} v_2(t)dt - S = \Delta S_j \quad \textbf{(2-22)}$$

In such a case, the spacing of object B_i would exactly match that of object B_j. In practice, because of the random initial spacings and the natural variability associated with τ_1, the times at which objects B_i or B_{i-1} arrive on the 2nd conveyor can never be known in real time. Without information about arriving objects, the controller can not intentionally affect the spacing deviation of objects on the 2nd conveyor. As a result, it is essential that the buffering regulator does not act to exaggerate the spacing deviations of arriving objects. If processing the current object creates a large spacing deviation for the next object, processing that object could create an even larger deviation for the object after that. This phenomenon leads to the development of arrival stability (AS). The arrival stability is defined by the following condition,

$$c_{AS}(t) \equiv \frac{1}{N}\sum_{j} \Delta S_j \qquad \forall\, j \mid 0 < x_j < x_0 \qquad \textbf{(2-23)}$$

where N is the number of objects on the 2nd conveyor between the origin and x_0. The spacing constant c_{AS} is the moving average of spacing deviations within this range. Any given object may be spaced with a deviation of ΔS_j, but on average, the spacing should match the designed spacing S. To have a stable system, $c_{AS} \to 0$.

2.5. Effects of Position Detection and Errors

In order to accurately deliver the object B_j, ΔS_j must first be determined. This involves using the sensor mounted at x_0 to measure the arrival of objects B_j and B_{j-1}. As mentioned in Section 2.3, the distance traveled by the conveyor between sensor triggers is measured by an incremental encoder mounted to the 2nd conveyor. In theory, the spacing deviation can be calculated from Equation (2-24).

$$\Delta S_j = \int_{t_{0,j-1}}^{t_{0,j}} v_2(t)dt - S \qquad \textbf{(2-24)}$$

In practice the signal generated by BS #1 is not sufficient to directly determine $t_{0,j}$. If the object has a physical volume, the sensor will trigger when the object's front, rather than its center, crosses x_0 at time $t_{0,j}^{-}$, where the superscript "-" refers to which end of the object triggers the sensor. The signal will change again at time $t_{0,j}^{+}$, when the object's back crosses x_0. The length l_j is computed for object B_j from Equation (2-25). These variables are illustrated in Figure 2-10.

$$l_j = \int_{t_{0,j}^{-}}^{t_{0,j}^{+}} v_2(t)dt \qquad \textbf{(2-25)}$$

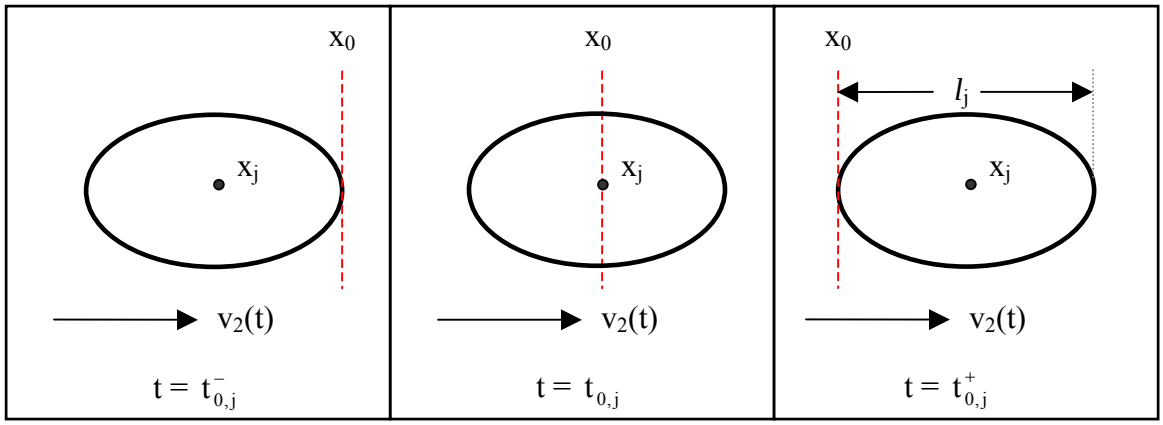

Figure 2-10: Schematic of Object Crossing BS #1

In this thesis we define the center to be the geometric midpoint between the object's front and back. The corresponding spacing deviation can then be calculated from Equation (2-26).

$$\Delta S_j = \int_{t_{0,j-1}^-}^{t_{0,j}^-} v_2(t)dt - \frac{l_j - l_{j-1}}{2} - S \qquad \textbf{(2-26)}$$

For position detection of a natural object using Equation (2-26), the calculated center may differ from the actual center. As a result the measured spacing deviation $\Delta\hat{S}_j$ differs from the actual spacing deviation ΔS_j by the measurement error $\varepsilon_{\Delta S_j} = \Delta\hat{S}_j - \Delta S_j$. For an improperly measured object, the calculation of an improper switch time $\hat{t}_s$ results in a path shown as Case 3 in Figure 2-5 has the same form as Equation (2-10):

$$\hat{t}_s = t_{f,j-1} + \frac{T(v_h - \bar{v}_2) - \Delta\hat{S}_j}{v_h - v_l} \qquad \textbf{(2-27)}$$

If $\varepsilon_{\Delta S_j} < 0$, then object B_j is actually further from the delivery point than measured. By changing speeds at $\hat{t}_s$, the object will be delivered after the end of the nominal cycle. For a small measurement error, $t_{f,j} > \hat{t}_s$, wherein B_j travels part of the total cycle distance at v_l until $t = \hat{t}_s$ and the remaining distance at v_h. For such a case, the relationship

between the error measurement and the timing error is derived as follows, using Equations (2-27), (2-7) and (2-8).

$$S + \Delta S_j = v_l(\hat{t}_s - t_{f,j-1}) + v_h(t_{f,j} - \hat{t}_s)$$

$$\bar{v}_2 T + \Delta S_j = v_l(\hat{t}_s - t_{f,j-1}) + v_h(\Delta t_j + t_{f,j-1} + T - \hat{t}_s)$$

$$v_h \Delta t_j = T(\bar{v}_2 - v_h) + (\hat{t}_s - t_{f,j-1})(v_h - v_l) + \Delta S_j$$

$$\Delta t_j = \frac{T(\bar{v}_2 - v_h) + (\hat{t}_s - t_{f,j-1})(v_h - v_l) + \Delta S_j}{v_h} \quad \textbf{(2-28)}$$

For a positive timing error, the expected tracking error for object B_j is calculated in Equation (2-29),

$$e_j = \int_{t_{f,j-1}+T+\tau_2}^{t_{f,j}+\tau_2} v_3(t)dt \quad \textbf{(2-29)}$$

which reduces to Equation (2-30) if the 3rd conveyor operates at a constant velocity:

$$e_j = \Delta t_j v_3 \quad \textbf{(2-30)}$$

2.6. Summary

A buffering regulator has been developed as a means to accurately deliver randomly spaced objects according to a demanded output spacing and throughput. The regulator will be judged both by its ability to meet the performance requirements and by the spacing variations it can withstand. To be effective, the buffering regulator must be able to tolerate a limited range of initial spacings, deliver objects with minimal tracking error and operate for short cycle times.

The main advantage of using buffer regulation is its simplicity. All that is needed for implementation are two proximity sensors, an incremental encoder and a motion controller that can calculate t_s and switch between two speeds. The trade off is the bound on its initial spacing. By using only two fixed speeds to create a buffer, the system relies on a large velocity change and a small unusable cycle time in order to compensate for

large variations in initial spacing. If either $v_h \rightarrow v_l$ or $T_u \rightarrow T$, then the allowable spacing deviation $\Delta S_j \rightarrow 0$.

It is desired to know what initial variability the system can tolerate, with what magnitude of tracking accurately it can deliver objects and how stable the buffer regulation will be. Assessment of these performance measures requires the determination of the system parameters and the implementation of the regulator onto an experimental setup. It is necessary to determine the speeds and average spacing for 2nd conveyor that both meet the throughput requirement and minimize the effects of measurement errors. Additionally, the conveyor dynamics and processing times must be measured in order to determine the acceptable spacing bounds from Equation (2-17). Implementation requires programming the controller to measure the spacing deviations using Equation (2-26) and switching velocities according to Equation (2-10). These issues will be examined in detail in Chapter 3, which investigates the effects of the regulator and issues concerning implementation.

CHAPTER 3

EXPERIMENTAL PARAMETER DETERMINATION

3.1. Introduction

This chapter investigates implementation issues of the proposed buffering regulator. The key parameters of the system are determined based on the performance requirements. Algorithms necessary to perform position detection and buffer regulation are presented and an experimental setup is discussed. The chapter ends with a study of the effects of buffer regulation on the timing error of delivered objects.

3.2. Experimental Setup

The three-conveyor system is setup as shown in Figure 2-1, in which the 3rd conveyor contains five pallets used for object delivery. The parameters used in the setup are illustrated in Figure 3-1,

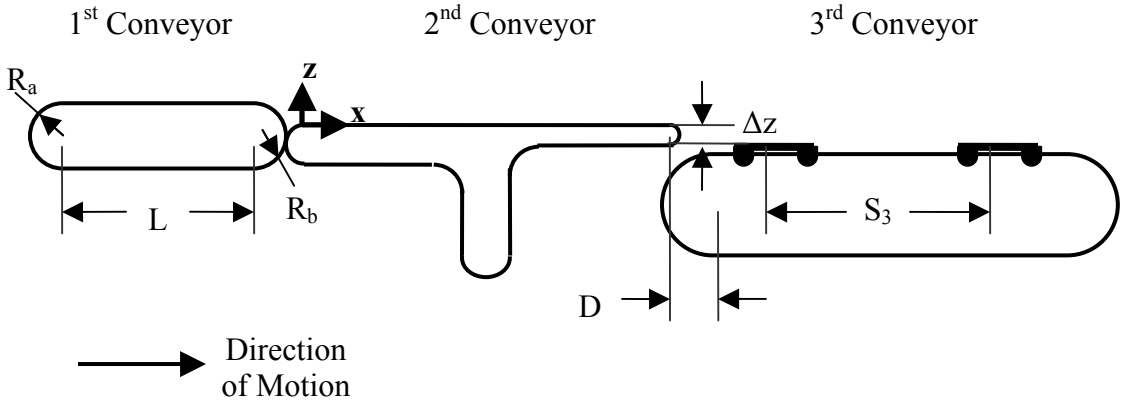

Figure 3-1: Side View of Experimental Setup

where R_a and R_b are the radii of curvature of the receiving and delivery ends of each conveyor respectively; L is the length of the flat conveyor surface; Δz is the height difference between the incoming and outgoing conveyor; D is the horizontal distance

between the incoming and outgoing conveyor; and S_3 is center-to-center distance between pallets. Values of these parameters are tabulated in Table 3-1.

Table 3-1: Conveyor Parameters

		1st Conveyor	2nd Conveyor	3rd Conveyor
L	(in)	66	109	88
Ra	(in)	2	1.5	7.5
Rb	(in)	2	0.75	7.5
Δz	(in)	–	0.5	1.75
D	(in)	–	4.5	1.0
S_3	(in)	–	–	36

The 1st (or loading) conveyor, on which objects arrive close-packed with random variations among their spacing and orientation, is driven by a DC brushless motor. The 2nd (or singulating) conveyor, which is driven by an AC motor, operates with an average speed greater than that of the loading conveyor. The speed difference ensures objects arrive on the 2nd conveyor with gaps wide enough for proper position detection. The 3rd (or separating) conveyor, driven by a DC brush motor, propels equally-spaced pallets at a constant speed. Position encoders mounted on each conveyor's output shaft measure 4000 counts per revolution. For the singulating conveyor, the resolution of distance measurements is found to be 330 counts/in.

The three conveyors are controlled by a Trio MC206 industrial motion coordinator. The Trio controller can simultaneously monitor the motion of all the conveyors and drum components, manage the beamswitch inputs, perform the calculations necessary for buffer regulation, and send command signals to each motor's amplifier. Additionally, the motion coordinator can record encoder and sensor information during operation for analysis. Some operating parameters of the Trio controller are tabulated in Table 3-2.

Table 3-2: Trio Controller Parameters

Parameter	Value
Servo/Stepper Axes	5
Position Resolution	32 Bit
Speed Resolution	32 Bit
24V I/O Channels	32
Analog Inputs	8
Analog Outputs	4
Servo Cycle	250 μs

The 1st and 3rd conveyors are commanded by Copley Xenus amplifiers with built-in microprocessors, which can store simple motion programs to execute given trajectories through position, velocity and current control. Some operating parameters of the Xenus Amplifiers are tabulated in Table 3-3.

Table 3-3: Xenus Amplifier Parameters

Parameter	Value
Mains Voltage	100-240 VAC
Mains Frequency	47-63 Hz
Continuous Current	20 A
Peak Current	40 A
Position Sample Time	333 μs
Velocity Sample Time	333 μs
Current Sample Time	67 μs
Analog Inputs	1
Digital Inputs	12
Digital Ouputs	3

The 2nd conveyor is commanded by a Toshiba G7 PWM Adjustable Speed Drive. The drive receives one of the two speed command signals from the controller and regulates the velocity through current and frequency control. Some operating parameters of the Toshiba Speed Drive are tabulated in Table 3-4.

Table 3-4: Toshiba Speed Drive Parameters

Parameter	Value
Voltage Rating	200-240 VAC
PWM Frequency	0.5-15 kHz
Freq. Cmnd. Resolution	0.1 Hz
Max. Short Circuit Current Rating	200,000A RMS
Analog Inputs	4

The two proximity beamswitches are Banner MINI-BEAMS®. The beamswitch monitors a beam of light between an emitter and a receiver mounted across the width of the singulating conveyor and outputs a digital signal indicating whether the beam is broken. It is assumed that objects are spaced such that the beamswitch can distinguish one object from the next. Additionally, the height at which the beamswitches are mounted should align as closely as possible with height of the average geometric center of the objects. A schematic of the system components is shown in Figure 3-2.

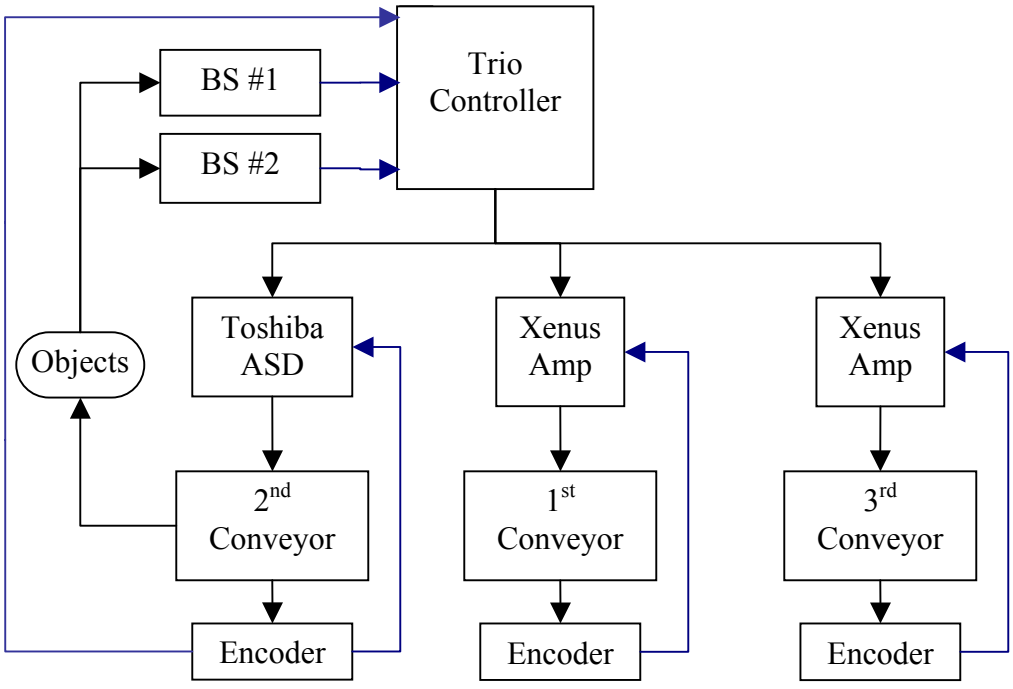

Figure 3-2: Schematic of System Components

3.3. Parameter Determination

To determine a steady-state operating condition, the nominal values of the conveyor parameters are determined experimentally. There are four variables of interest from which these parameters are determined:

1) The average velocity $(\bar{v}_2)$
2) The velocity range $(v_h - v_l)$
3) The measurement error $(\varepsilon_{\Delta S_j})$
4) The timing error (Δt_j)

In addition, we discuss the design considerations in relation to practical implementation of the buffer regulation algorithm. These considerations are outlined as follows.

Effects of Velocity Range on Spacing Bounds: In Equation (2-17), the spacing bounds are a function of the usable cycle time and the velocity range. In this section, the constraints imposed upon the velocity range necessary to maximize the acceptable spacing range are discussed.

Effects of Velocity Changes on Live Objects: In this section, the constraints imposed on the velocity range are discussed in relation to maintaining the assumptions given in Chapter 1. In particular, the effects of velocity changes on live object location are discussed.

Effects of Measurement Errors on Timing Errors: Equation (2-28) presents a mathematical relationship between measurement errors and expected timing errors. This section analyzes this relationship to determine constraints imposed upon the velocity range and average speed to minimize the effects of measurement errors.

3.4. Effects of Velocity Range on Spacing Bounds

It is desired to maximize the range of tolerable spacings because this determines how much natural variation the system can handle. If the bounds are too narrow, only objects with minor initial spacing deviations can be accurately delivered. The error reduction effects of such a system would be negligible. A system that can accommodate a large range of initial spacing deviations, however, is of much value in manufacturing.

The tolerable spacing bounds are determined from Equation (2-17) for a specified T, where T_u is a constant based on the system hardware. For a given T_u, Equation (2-17) shows that (1) there is a direct linear relationship between $(v_h - v_l)$ and ΔS_j. (2) The larger the gap between speeds, the larger a spacing deviation the buffer regulation can handle. The spacing bound is independent of $\bar{v}_2$. From this result, the conveyor speeds should be chosen to create the greatest velocity change in order to maximize the spacing bounds.

3.5. Effects of Velocity Changes on Live Objects

It is desired to tune the 2nd conveyor in order to minimize T_r such that T_u can be reduced so more of the cycle time can be used for buffer regulation. However, the faster $v_2(t)$ switches from v_h to v_l, the larger the acceleration becomes that will be imparted to the objects on the 2nd conveyor. While processing live animals, the objects must stay balanced in order to maintain their position. Even while processing inanimate objects, the acceleration force must not be enough to overcome static friction or topple the objects.

The acceleration felt by the object will be proportional to the velocity range. To keep objects from shifting, the range should be narrow. However, keeping objects in place is directly at odds with increasing the spacing bounds. It was found that the velocity range should be as wide as possible to accommodate large initial variations. A compromise must be reached to satisfy both requirements.

3.6. Effects of Measurement Errors on Timing Errors

Due to measurement errors, the choice of v_h and v_l could affect the timing errors. As shown in Equation (2-28), the expected timing error is a function of T, $\varepsilon_{\Delta S_j}$, v_h and v_l. For a given cycle time and measurement error, it is desired that the choice of conveyor velocities not exaggerate the effect on delivery time. The timing errors are simulated for three different cases, in all of which the measurement error $\varepsilon_{\Delta S_j}$ is varied from 0 to 0.5 in. The parameters for these cases are listed in Table 3-5 and the simulated effects of measurement errors on the timing error are shown in Figure 3-3 through Figure 3-5 for Cases #1-3 respectively.

Table 3-5: Parameters for Simulation of Measurement Error Effects

	$v_h - v_l$ (in/s)	$\bar{v}_2$ (in/s)	Common
Case #1	8	4 to 16	$T = 4/3$ s $v_1 = 10$ in/s $v_3 = 27$ in/s $\tau_2 = 0$
Case #2	1 to 10	10	
Case #3	$2\bar{v}_2$ if $\bar{v}_2 \le 10$ $20 - 2\bar{v}_2$ if $\bar{v}_2 > 10$	1 to 19	

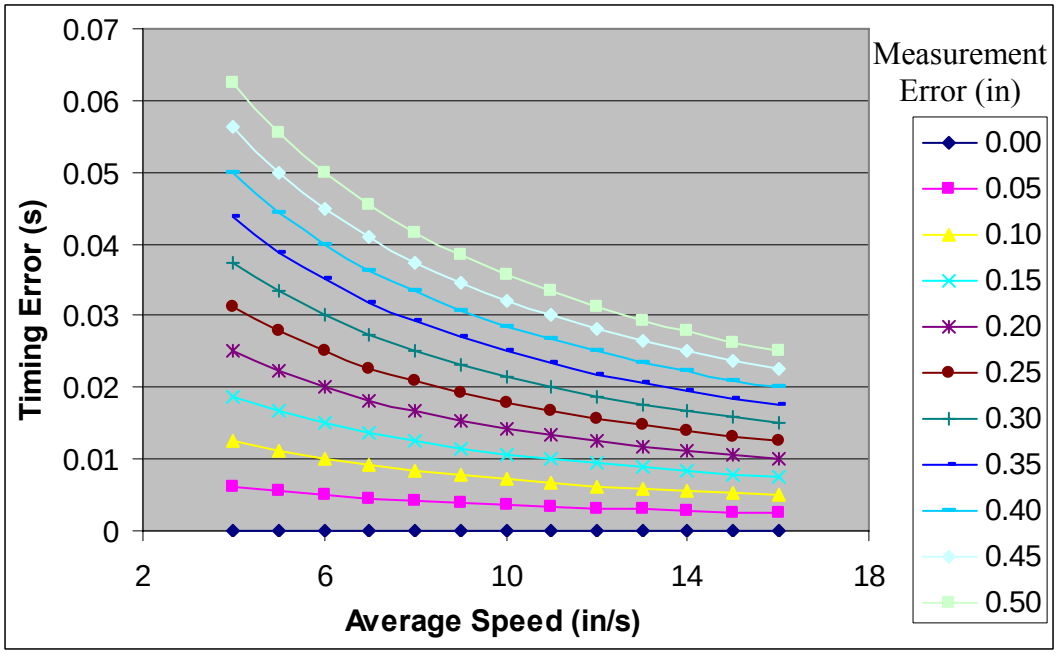

Figure 3-3: Timing Errors for Constant Velocity Range

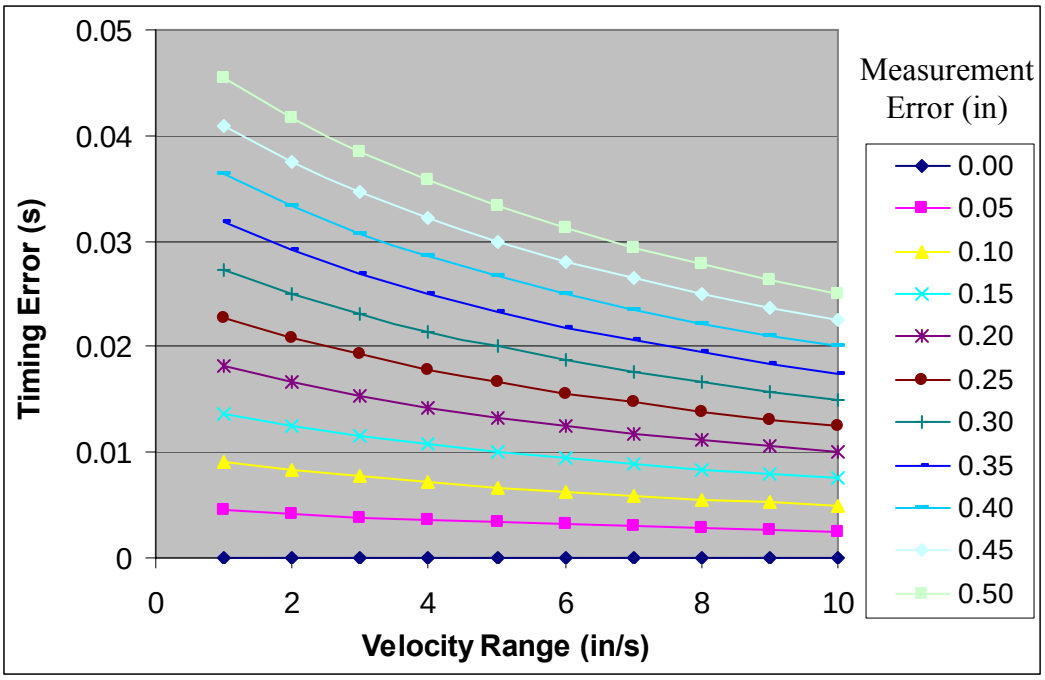

Figure 3-4: Timing Errors for Constant Average Speed

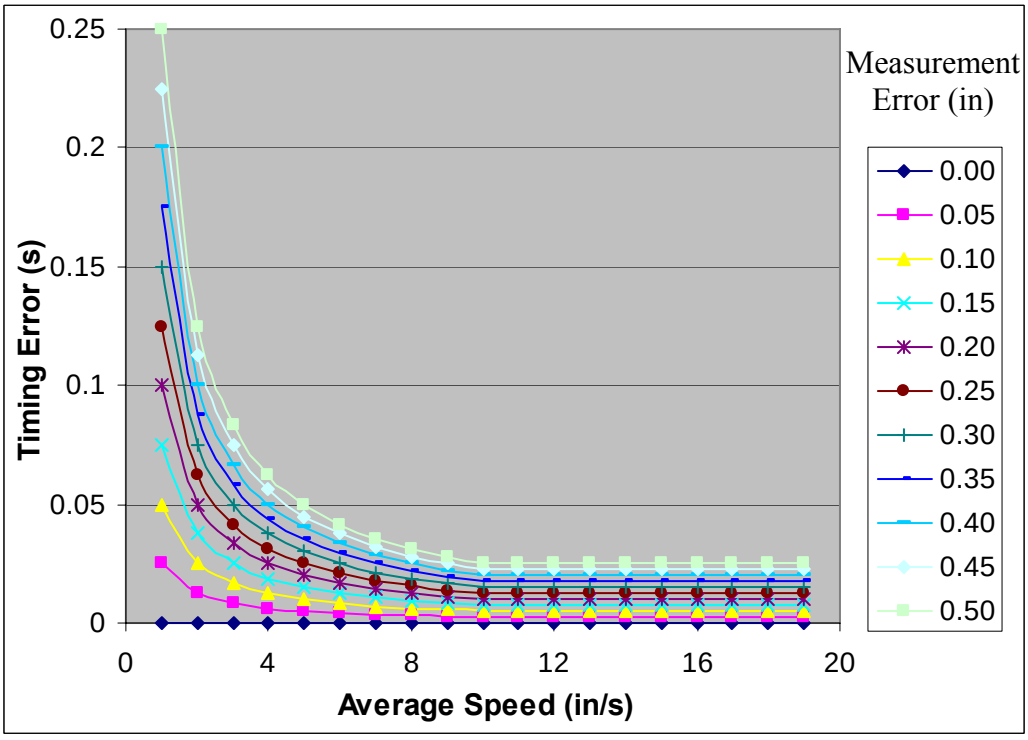

Figure 3-5: Timing Errors for Maximum Velocity Range

In Case #1, $(v_h - v_l)$ is kept at a constant of 8 in/s. Timing errors are plotted against $\bar{v}_2$ for specified measurement errors. Figure 3-3 shows that timing errors can be reduced by using a higher average velocity. In Case #2 where $\bar{v}_2$ is kept at 10 in/s, the timing errors are plotted against $(v_h - v_l)$. As shown in Figure 3-4, the timing error reduces as the velocity range increases. In Case #3, where $(v_h - v_l)$ is maximized within the range 0 – 20 in/s, the timing errors are plotted against $\bar{v}_2$. As shown in Figure 3-5, the timing error is substantially reduced as the range and average velocity increase. However, for $\bar{v}_2 > 10$ in/s, the effects of decreasing the range cancel the effects of increasing average velocity, resulting in no timing error change.

The results indicate that the effects of measurement errors on timing errors can be minimized by the use of a large $\bar{v}_2$ and $(v_h - v_l)$. However, if the velocity is bounded, increasing the average velocity past the median allowable speed necessitates the reduction of the range, causing no net improvement in timing error reduction.

Velocity Selection

There also exist two physical constraints upon the velocity selection imposed by the experimental setup described as follows:

1. The speed of the 2nd conveyor is bounded: $0 < v_2(t) \leq 20$ in/s.
2. Processes handled by the 3rd conveyor will perform better if objects arrive upon it at a similar velocity. Because objects transfer to the 3rd conveyor at the end of their buffering cycle, they arrive at the speed v_h. To meet this constraint, the difference between v_3 and v_h should be minimized.

All of the factors affecting velocity selection are summarized in Table 3-6 along with the final selection that offers an optimal tradeoff. With $\bar{v}_2$ set, the average spacing S is calculated from Equation (2-8).

Table 3-6: Velocity Selection Factors

Desired Effect	Design Conditions			
	$\bar{v}_2$	$v_h - v_l$	v_h	v_l
Spacing Bounds	–	Maximize	–	–
Timing Error	Maximize	Maximize	–	–
Live Object Reaction	–	Minimize	–	–
Velocity Limits	–	–	≤ 20 in/s	≥ 0 in/s
Transition to 3rd Conveyor	–	–	→ 27 in/s	–
Final Selection	**16**	**8**	**20**	**12**

3.7. Algorithm

The buffer regulation algorithm consists of two routines, position detection and buffer regulation. Implementation of the algorithm requires that the controller monitor multiple objects and shift its attention to the next object once the current object has been delivered. Figure 3-6 shows a flow chart of the tasks necessary to implement this algorithm. The left path of the Figure 3-6 performs position detection and the right path performs buffer regulation. The counter i for the left path should always be equal to or greater than the counter j for the right path because the beamswitches are located such that at least two objects pass through BS #1 before any reach BS #2. If this were not the case, as one object is delivered, the next cycle could not begin because the next object's spacing deviation would not have been calculated. If the system processes all the objects, $j - i = 1$ and the algorithm terminates. The two routines are explained below.

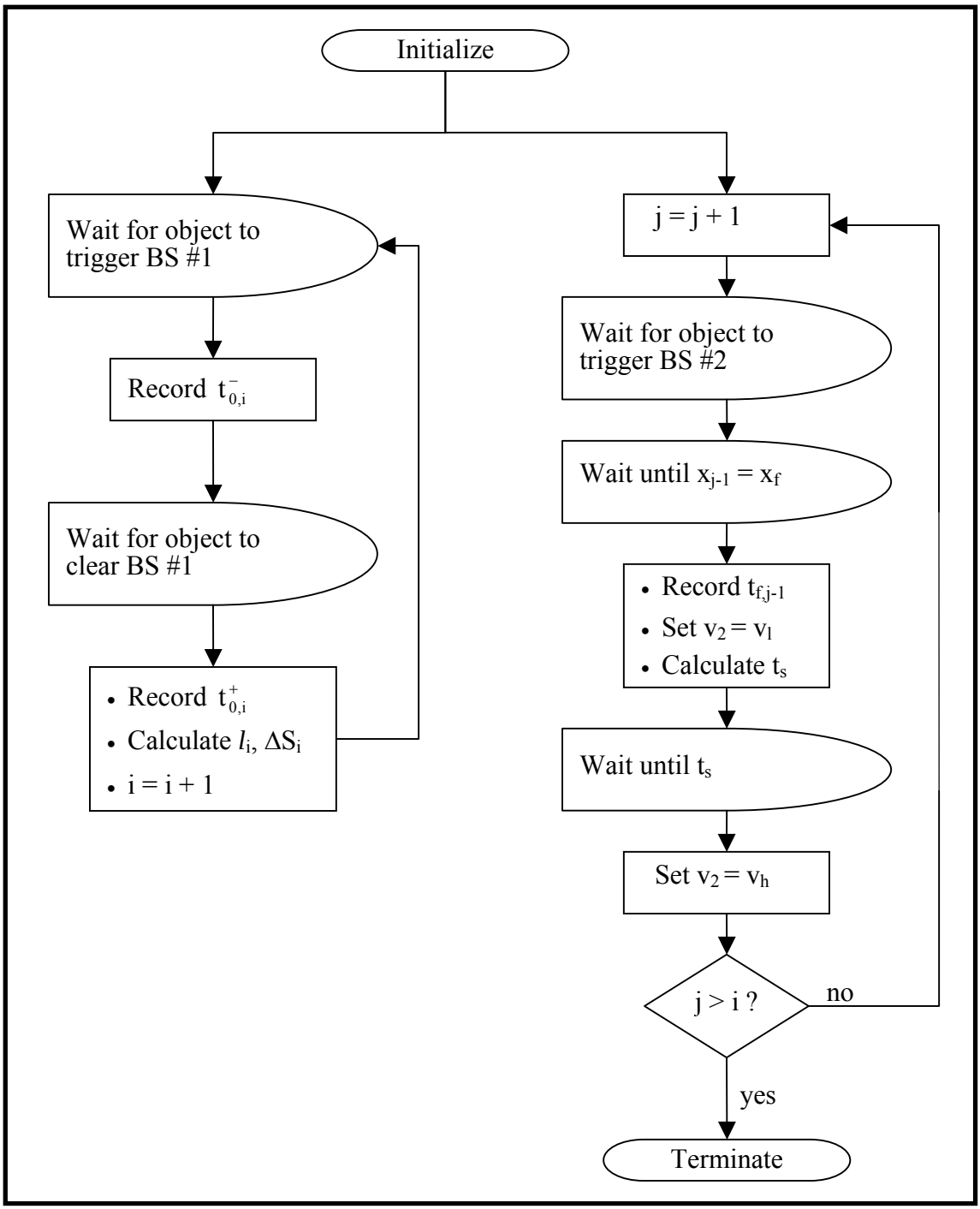

Figure 3-6: Flowchart of Complete Buffer Regulation Algorithm

Position Detection Routine

This routine uses BS #1 to detect the incoming object on the 2nd conveyor. The beamswitch signal initializes the encoder to determine the location of the incoming object with respect to x_0. The length and spacing deviation are calculated using Equations (2-25) and (2-26) respectively. For the i^{th} object approaching x_0, the routine operates as follows:

1. Wait for BS #1 to trigger. Record $t_{0,i}^{-}$ once it is triggered.
2. Wait for BS #1 to clear. Record $t_{0,i}^{+}$ once it is cleared
3. Calculate l_i from Equation (2-25).
4. Calculate ΔS_i Equation (2-26).
5. Increment the counter i.
6. Go to step 1.

Buffer Regulation Routine

This routine uses the position detection results and the signal from BS #2 to calculate t_s and adjust $v_2(t)$ accordingly. It requires that the length and spacing deviation of object B_j are stored in the controller's memory. The routine begins as B_{j-1} approaches BS #2; the 2nd conveyor should be operating at v_h from the end of the previous cycle.

1. Wait until the front of object B_{j-1} triggers BS #2.
2. Wait until the conveyor has moved $l_{j-1}/2$, at which point the center of B_{j-1} should reach x_f. Record $t_{f,j-1}$.
3. Change the 2nd conveyor's velocity to v_l.
4. Calculate t_s using Equation (2-10).
5. Wait until t_s, and then switch to v_h.
6. Increment the counter j.

7. Go to step 1.

This routine repeats for as long as necessary to process all objects. When the last object passes through BS #2, the controller will have no information available in its memory to perform step 2. By recording the delivery time t_{fj}, the timing error can be calculated in real-time.

3.8. Experimental Determination of Conveyor Characteristic Times

To account for the dynamics of the conveyors, the characteristic time T_r of the conveyors is obtained experimentally. For each conveyor, its incremental encoder is first calibrated by moving the conveyor a known distance and counting the corresponding number of encoder clicks. Then, the conveyor receives a step velocity input while loaded with weights equivalent to the mass it is expected to transport during operation. The normalized responses obtained experimentally are shown in Figures 3-8 through 3-12 for the three conveyors.

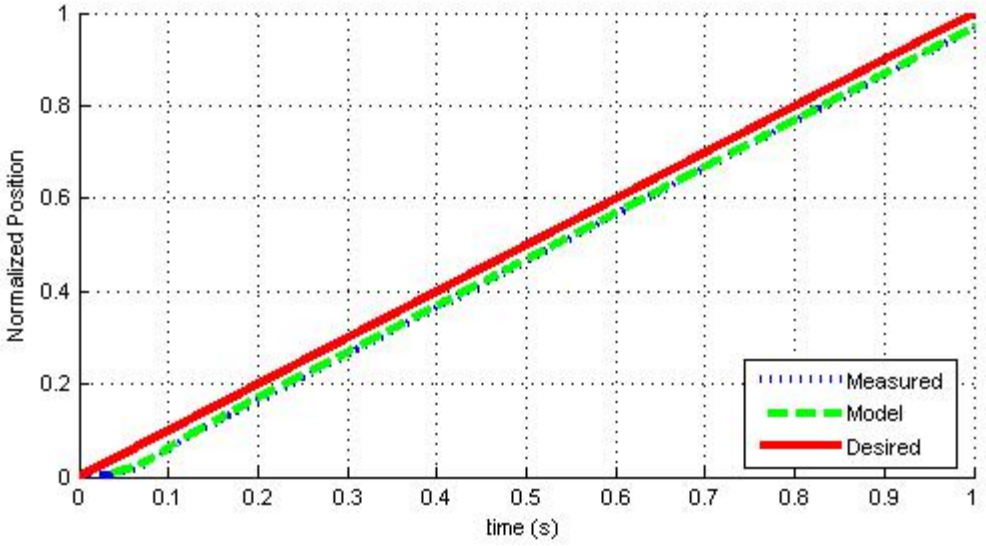

Figure 3-7: Loading Conveyor Position Response

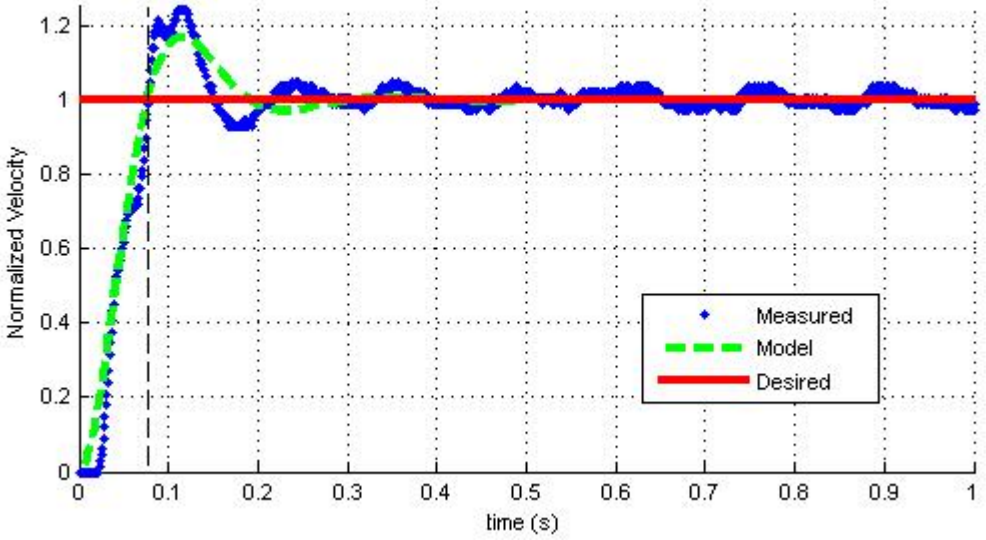

Figure 3-8: Loading Conveyor Velocity Response

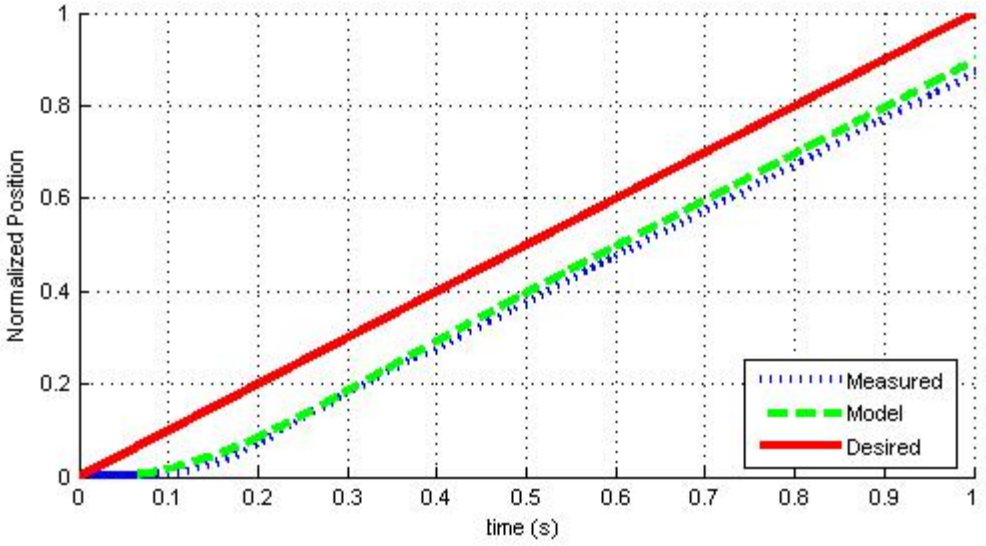

Figure 3-9: Singulating Conveyor Position Response

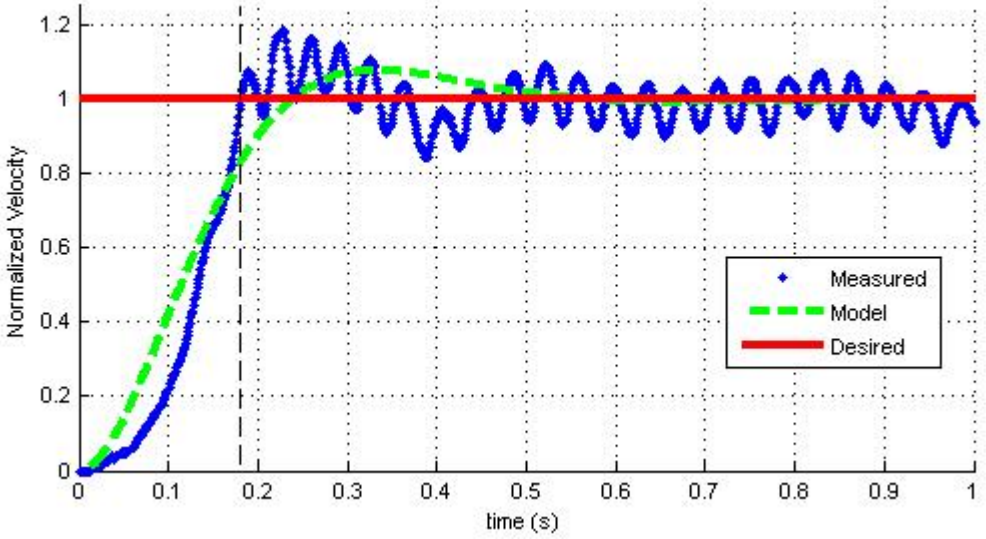

Figure 3-10: Singulating Conveyor Velocity Response

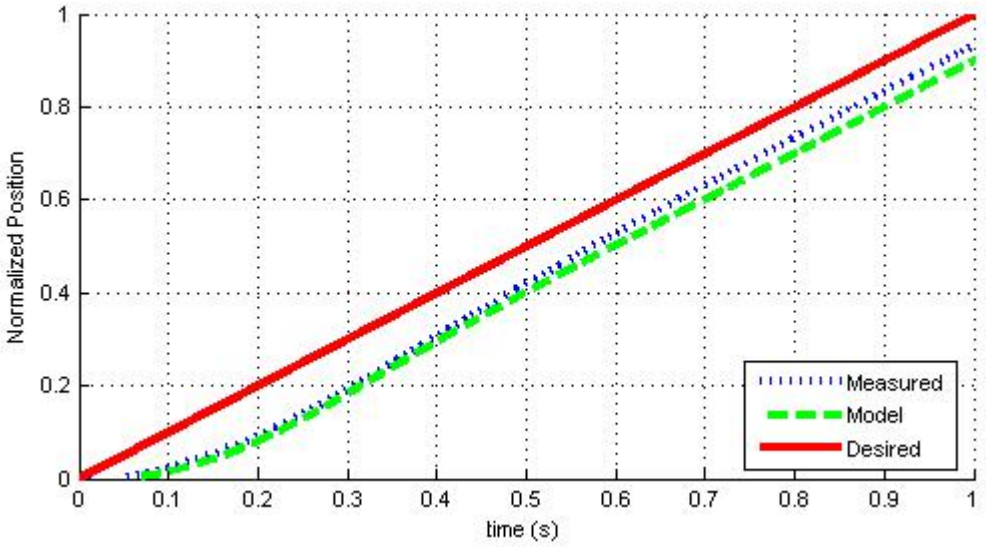

Figure 3-11: Separating Conveyor Position Response

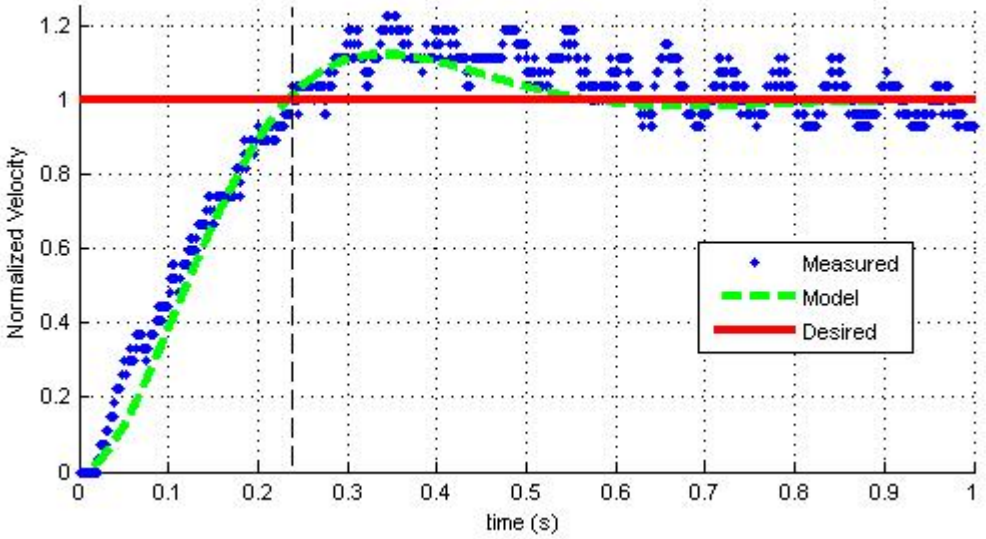

Figure 3-12: Separating Conveyor Velocity Response

The data show that the step responses can be characterized by a 2nd order system model of the form

$$H(s) = \frac{\omega_n^2}{s^2 + 2\zeta\omega_n s + \omega_n^2} \qquad \textbf{(3-1)}$$

A least squares fit of the model to the data produced the parameters tabulated below in Table 3-7, accompanied by the commanded speeds and characteristic times.

Table 3-7: Experimental Conveyor Parameters

Conveyor	**Commanded Speed** (in/s)	ζ	ω_n	T_r (s)
Loading	10	0.493	31.45	0.077
Singulating	16	0.631	12.13	0.180
Separating	27	0.555	11.10	0.238

3.9. Experimental Determination of Processing Times

The remaining system parameters to determine are the variables in Equation (2-15) that dictate the unusable cycle time. T_r has already been measured to be 0.180 seconds as shown in Table 3-7 and the effect of τ_2 not considered. The processing times T_{pd} and T_{br} are determined by running the respective routines on the controller through many iterations. The processing time per cycle equals the division of the total time by the number of iterations. For this test, 100,000 cycles were run on each routine. The results are tabulated in Table 3-8. It is expected that a total of 1.238 ms of processing time will be used per object.

Table 3-8: Processing Times

Operation		**Time per cycle (ms)**
Position Detection	T_{pd}	0.49614
Buffer Regulation	T_{br}	0.74193
Sum		**1.23807**

The final value needed is the time required to operate the beamswitches. The scan time T_{bs} is proportional to the number of light beams per sensor. As mentioned in Section 3.2, the beamswitches only monitor a single beam to detect objects, requiring a scan time of 0.11 ms [Banner]. In Chapter 4, a more advanced position detection algorithm will be discussed that requires more beams and as a result, a larger T_{bs}. A minimum of three scans are necessary to process a single object: BS #1 requires one scan to locate the object's front, one to locate its back, and BS #2 also requires one to locate

the object's front. Therefore, n = 3 for the experimental setup. Taken together, the total amount of unusable time per cycle T_u is calculated in Table 3-9.

Table 3-9: Calculation of Unusable Cycle Time

Operation	Time (ms)
Deceleration	180
Acceleration	180
Controller Processing	1.24
3 x Sensor Scans	0.33
τ_2	0
T_u	**361.57**

Once T_u is known, the actual spacing bounds can be determined using Equation (2-17) and the values of T from Table 3-5, and v_l and v_h from. The acceptable spacing bounds are tabulated in Table 3-10, where the theoretical spacing bounds are calculated from Equations (2-13) and (2-14).

Table 3-10: Experimental Spacing Bounds

	Lower Bound (in)	Upper Bound (in)
Theoretical	16.00	26.67
Actual	17.45	25.22

If the system were processing birds, the actual range would be longer than the average bird's torso. For such an application, this range should provide a suitable tolerance to account for the initial spacing variations.

3.10. Buffering Regulation Simulations

It is desired to study how the initial conditions will affect the system performance. One of the main obstacles to proper delivery arises from the uncertainty in the initial spacing of the arriving object, $S_1 + \delta S_j$. If the magnitude of δS_j is too great, object B_j will arrive on the 2nd conveyor with ΔS_j outside of the acceptable range. Similarly, S_1 and v_1 should relate such that objects are delivered according to the demanded throughput, just like spacing and speed of the 2nd conveyor are related in Equation (2-8). It is expected

that if there is a mismatch between the actual and desired throughput, objects will not reach the singulating conveyor approximately once each cycle, and the spacing deviations will grow, eventually exceeding tolerance. A simulation is created for this purpose.

The simulation consists of N objects traveling from initial locations on the loading conveyor through x_f for I iterations. Since the focus here is the effects of initial spacing, the $S_1 + \delta S_j$ is chosen randomly from a normal distribution of mean S_1 and standard deviation σ_1. The ΔS_j is calculated directly from Equation (2-21) rather than through the position detection routine, so there are no measurement errors. The buffer regulation routine is implemented to calculate t_s from Equation (2-10) based on the known spacing deviation. During buffer regulation, it is guaranteed that any object with tolerable spacing deviation will be delivered with no timing error.

The relative spacing variability of objects on a conveyor is calculated in Equation (3-2),

$$\text{Relative Variability} = \frac{\hat{\sigma}_i}{\hat{S}_i} \qquad \text{for } i = 1,2 \tag{3-2}$$

where $\hat{S}_i$ is the measured mean spacing of objects on the i^{th} conveyor and $\hat{\sigma}_i$ the measured standard deviation. For a given initial conveyor speed v_1, the percentage of mismatch between the initial throughput and the desired throughput is calculated from (3-3).

$$\% \text{ Mismatch} = 100\left(1 - \frac{S_1}{v_1 T}\right) \tag{3-3}$$

S_1 is set at 7.5 in. However, for different tests with the same σ_1, the initial object spacing will not be identical due to random selection. Three different cases, summarized in Table 3-11, are simulated and the results plotted in Figures 3-13 through 3-16.

Table 3-11: Buffer Regulation Simulation Parameters

Cases #	I	N	σ_1 (in)	% Mismatch	v_2
1	300	10	0.25	[0, 10, 20]	Nominal
2	425	10	0.2 to 1.0	0	Buffering
3	11	20	0	0 to 5	Buffering

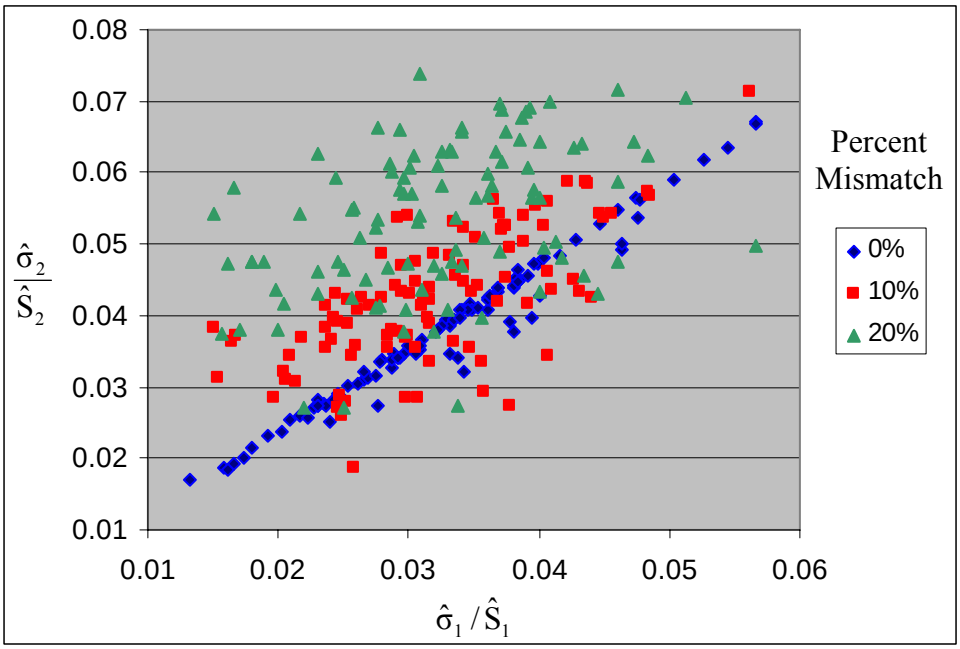

Figure 3-13: Relative Variability Across Conveyors

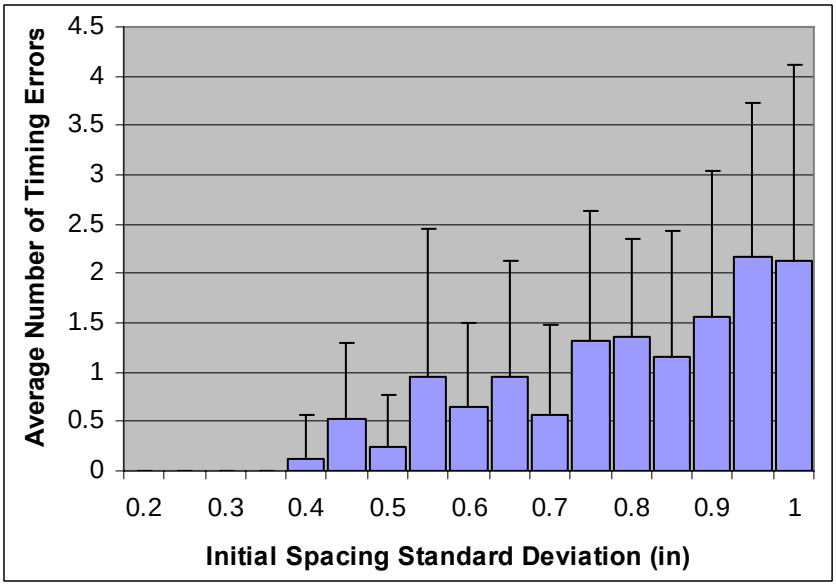

Figure 3-14: Number of Timing Errors per Test vs σ_1

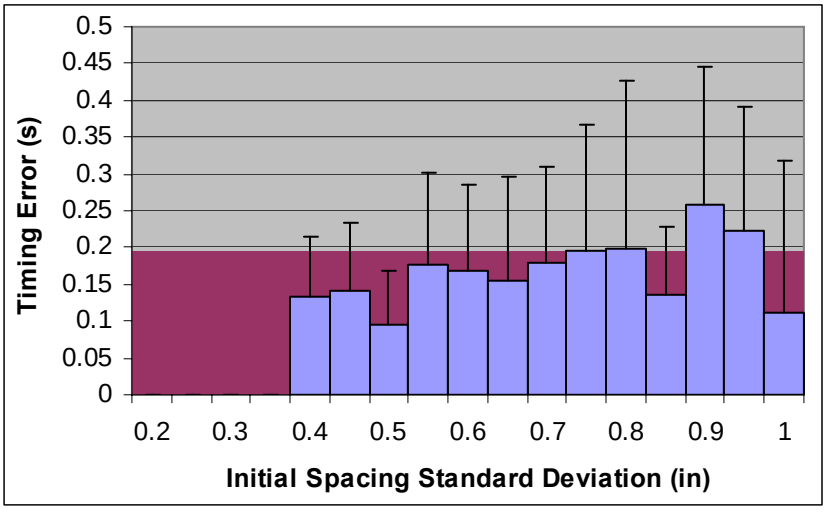

Figure 3-15: Average Timing Error for Tests in which Errors Occurred.

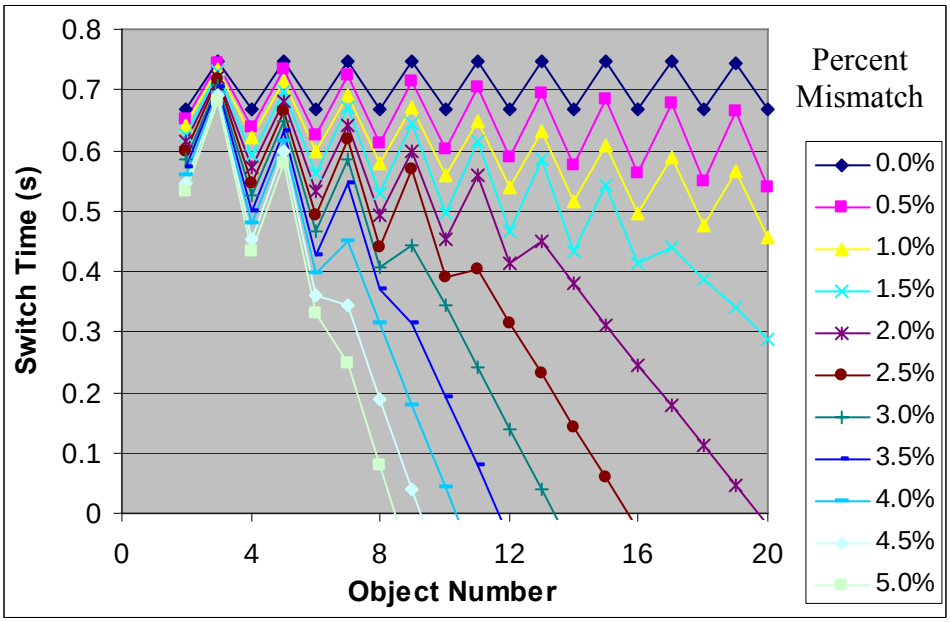

Figure 3-16: Switch Time vs Object Number for Increasing % Mismatches

In Case #1, σ_1 is kept at a constant of 0.25 in. while $\hat{\sigma}_2 / \hat{S}_2$ is plotted against $\hat{\sigma}_1 / \hat{S}_1$ for three different % mismatches. Figure 3-13 shows that for low % mismatches, there is a very predictable, linear relationship between the object spacing on the 1st and 2nd conveyors. As the % mismatch increases, the correlation is reduced.

In Case #2, the % mismatch is eliminated, and the average number and magnitude of timing errors are plotted against a range of σ_1. Figure 3-14 shows that the average

number of objects delivered with timing errors increases with σ_1. There exists a standard deviation less than which all objects will be delivered on time. Figure 3-15 shows that the average magnitude of timing errors (presented as columns) is not significantly affected by σ_1 and that the standard deviation of timing errors (presented as bars) is affected. For objects that have the same length as the pallet, the red bar in Figure 3-15 represents the maximum timing error that would result in an object at least partially landing on the pallet. For timing errors above that line, the object would miss the pallet completely. The results indicate that when timing errors occur, they have a high probability of resulting in unacceptable tracking errors.

In Case #3, the switch time of objects with perfect spacing is plotted against a range of % mismatches. Figure 3-16 shows that the system will become unstable over time if any % mismatch exists, with failure occurring sooner for larger mismatches. Theoretical failure is indicated by a switch time at or below zero (or above T). In practice, failure occurs if the switch time lies in the unusable part of the cycle. When there is no percent mismatch, the system is AS stable as defined in Equation (2-23). The oscillations present in Figure 3-16 are the result of a disparity between the times the objects arrive on and leave the singulating conveyor.

3.11. Discussion and Summary

The results from this simulation indicate three clear trends:

1) As the percent mismatch increases, the spacing variability of objects on the 2nd conveyor increases. A larger variability creates a greater probability that spacing deviations will lie outside of the acceptable bounds, eventually leading to improper delivery.
2) Larger initial spacing standard deviations create more, though not necessarily larger, timing errors. When timing errors occur, they will often result in complete delivery failures.

3) Even for objects with perfect initial spacing, if the throughputs do not match, failure is inevitable.

Taken together, these three simulations provide very strict requirements on the loading conveyor. In short, it is necessary to match its throughput with the desired value and ensure that the initial variability is small. If either of these rules is broken, the system will inevitably deliver improperly spaced objects.

In this chapter, the principle components of the experimental setup concerning the implementation of the buffer regulation algorithm are discussed. An algorithm for position detection and buffer regulation is presented. A series of tests are performed to acquire the necessary system parameters and a simulation is performed to examine the performance of the system for different initial conditions. The next chapter will experimentally investigate the effects of the buffer regulation algorithm.

CHAPTER 4

EXPERIMENTAL RESULTS

4.1. Introduction

In the previous chapter, a means to implement the buffer regulation algorithm was presented, including the experimental setup and necessary algorithms. A series of tests and simulations were performed to determine the system parameters and identify potential problems. In this chapter, the buffer regulation algorithm is implemented onto the experimental setup and its performance analyzed. Specifically, the following experiments have been conducted to evaluate the performance of the buffer regulator:

Position Detection Performance: This experiment evaluated the ability of BS #1 and the controller to measure the object length l_j and the spacing deviation ΔS_j using the position detection routine. The expected measurement errors have been determined for a known object.

Single Conveyor Buffer Regulator Performance: This experiment evaluated the performance of the buffer regulator to compensate for the spacing deviations of a set of objects containing different types of spacings along the length of a single conveyor. Timing errors have been recorded for different types of objects when the initial spacing is both known and when it is determined using the position detection routine.

Two-Conveyor Buffer Regulator Performance: This experiment evaluated the performance of the buffer regulator to compensate for the spacing deviations of objects traveling across two conveyors. Timing errors have been recorded for two different locations of BS #1.

Three-Conveyor Buffer Regulator Performance: This experiment evaluated the performance of the buffer regulator to deliver randomly-spaced objects on the 1st conveyor onto the pallets of the 3rd conveyor. For a range of initial spacings, the spacing deviations, tracking errors and delivery state were recorded.

These experiments are performed using the common parameters from Table 3-5.

4.2. Position Detection Performance

An experiment was conducted to evaluate the performance of the position detection routine. It is desired to know how accurately the length and spacing of well defined objects could be measured based on the magnitude of measurement errors produced. The experimental setup is shown in Figure 4-1 and the parameters are tabulated in Table 4-1.

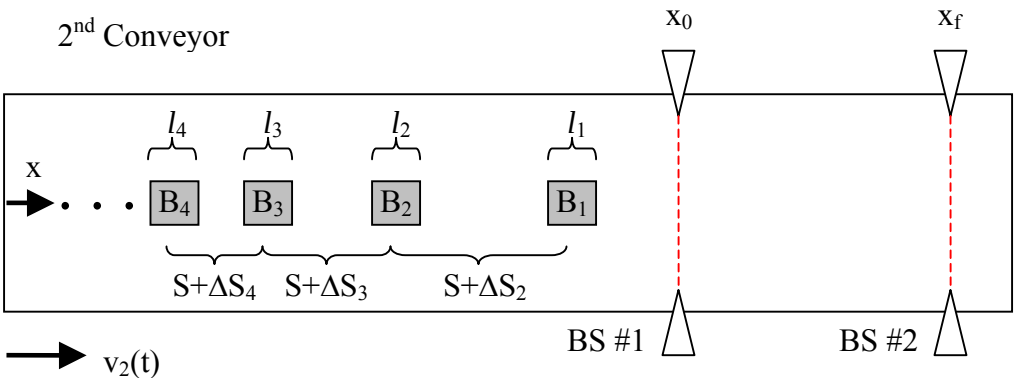

Figure 4-1: Plan View of Experimental Parameters

Table 4-1: Experimental Parameters for Position Detection

Parameter	Value
N	4
I	12
l_j	4 cm, ∀j
$S+\Delta S_2$	8.89 in
$S+\Delta S_3$	5.15 in
$S+\Delta S_4$	6.61 in
$v_2(t)$	5 in/s
x_0	60 in

In this test, N objects of uniform length were placed on the 2nd conveyor with known spacings $S+\Delta S_j$. Care was taken to ensure that the objects were oriented such their sides were parallel to the direction of motion. Once the objects were positioned correctly, the conveyor moved forward at $v_2(t)$. The initial placement of the objects and of BS #1 ensured that the conveyor will reach steady state before B_1 reaches x_0. For the conditions given above, 12 iterations were performed, recording the measured length and spacing of each object. The results are tabulated below in Table 4-2, where $\varepsilon_{l_j} = \hat{l}_j - l_j$ and $\varepsilon_{\Delta S_j} = \Delta\hat{S}_j - \Delta S_j$ denote the length and spacing measurement errors of object B_j respectively.

Table 4-2: Measurement Errors from Position Detection of Uniform Objects

	$\boldsymbol{\varepsilon}_{l_j}$ (in)				$\boldsymbol{\varepsilon}_{\Delta S_j}$ (in)		
I	**j=1**	**2**	**3**	**4**	**2**	**3**	**4**
1	0.048	0.057	0.139	0.057	-0.005	0.121	-0.137
2	0.027	0.121	0.233	0.066	0.140	0.173	-0.216
3	0.097	0.112	0.130	0.009	0.001	0.056	-0.187
4	0.075	0.145	0.148	0.094	0.043	0.027	-0.093
5	0.042	0.097	0.091	0.075	0.133	0.026	-0.043
6	0.024	0.091	0.103	0.057	0.042	0.035	-0.067
7	0.030	0.075	0.094	0.121	-0.026	0.044	0.024
8	0.051	0.145	0.130	0.078	0.180	0.021	-0.046
9	0.069	0.097	0.085	0.012	0.043	-0.068	-0.066
10	0.039	0.069	0.121	0.109	0.017	0.006	-0.011
11	0.130	0.139	0.097	0.133	-0.005	-0.059	-0.008
12	0.085	0.163	0.115	0.021	0.102	-0.029	-0.134
	$\overline{\boldsymbol{\varepsilon}}_{\boldsymbol{l}}$				$\overline{\boldsymbol{\varepsilon}}_{\Delta S_2}$	$\overline{\boldsymbol{\varepsilon}}_{\Delta S_3}$	$\overline{\boldsymbol{\varepsilon}}_{\Delta S_4}$
Average	0.091				0.062	0.055	0.086
Std. Dev.	0.045				0.061	0.048	0.069

The average measurement errors in the length and the spacing of object B_j are calculated respectively from Equations (4-1) to (4-2),

$$\overline{\varepsilon}_{l_j} = \frac{1}{I}\sum_{i=1}^{I}\left|\hat{l}_j - l_j\right| \quad \textbf{(4-1)}$$

$$\overline{\varepsilon}_{\Delta S_j} = \frac{1}{I}\sum_{i=1}^{I}\left|\Delta\hat{S}_j - \Delta S_j\right| \quad \textbf{(4-2)}$$

where I is the number of iterations. The average measurement error over all object lengths is given in Equation (4-3)

$$\bar{\varepsilon}_l = \frac{1}{N}\sum_{j=1}^{N} \bar{\varepsilon}_{l_j} \tag{4-3}$$

where N is the number of objects per iteration.

It can be seen that all of the mean errors are below 0.1 inches. From Figure 3-3, the spacing measurement error less than 0.1 in. corresponds to a timing error under 0.05 seconds, or a tracking error less than 1.8 in., calculated from Equation (2-30).

4.3. Single-Conveyor Buffering Regulator Performance

Two preliminary tests of the buffering regulator have been performed to evaluate its ability to deliver objects according to the required throughput. It is desired to learn how the type of object, spacing deviation and use of position detection affect the timing error. For these tests, the 2nd conveyor was configured for the setup shown in Figure 4-1. The velocity trajectory operated with v_l = 4 in/s and v_h = 8 in/s. BS #1 and BS #2 were located at x_0 = 50 in. and x_f = 100 in. respectively. The parameters for these tests are tabulated in Table 4-3 and the results of Test #1 are shown in Figures 4-2 through 4-5.

Table 4-3: Single-Conveyor Experimental Parameters

Test #		N	I	Object	ΔS_j Measure	$S+\Delta S_2$ (in)	$S+\Delta S_3$ (in)	$S+\Delta S_4$ (in)	$S+\Delta S_5$ (in)	$S+\Delta S_6$ (in)
1	(a)	4	1	Uniform Block	Manual	9.00	9.00	9.00	–	–
	(b)	3	1	Uniform Block	Manual	9.88	8.01	–	–	–
2	(a)	6	6	Football	Position Detection	~8.0	~8.0	~8.0	~8.0	~8.0
	(b)	4	5	Uniform Block	Position Detection	8.89	5.15	6.61	–	–

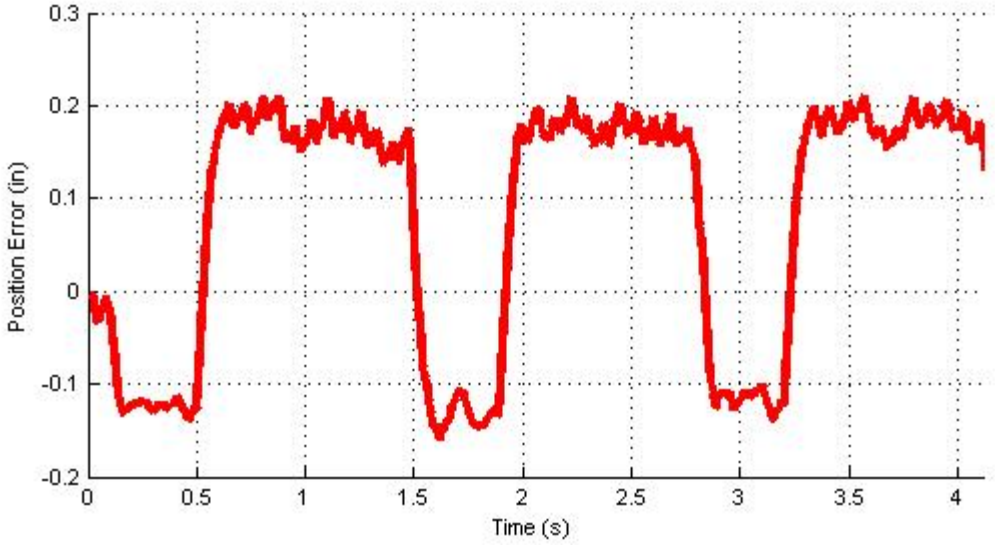

Figure 4-2: Position Error Results of Test #1 (a)

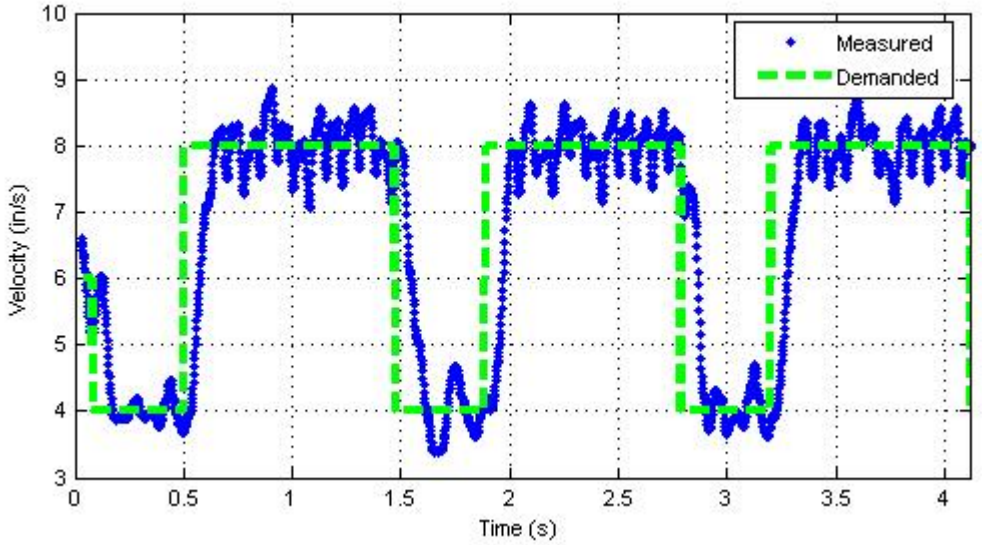

Figure 4-3: Velocity Results of Test #1 (a)

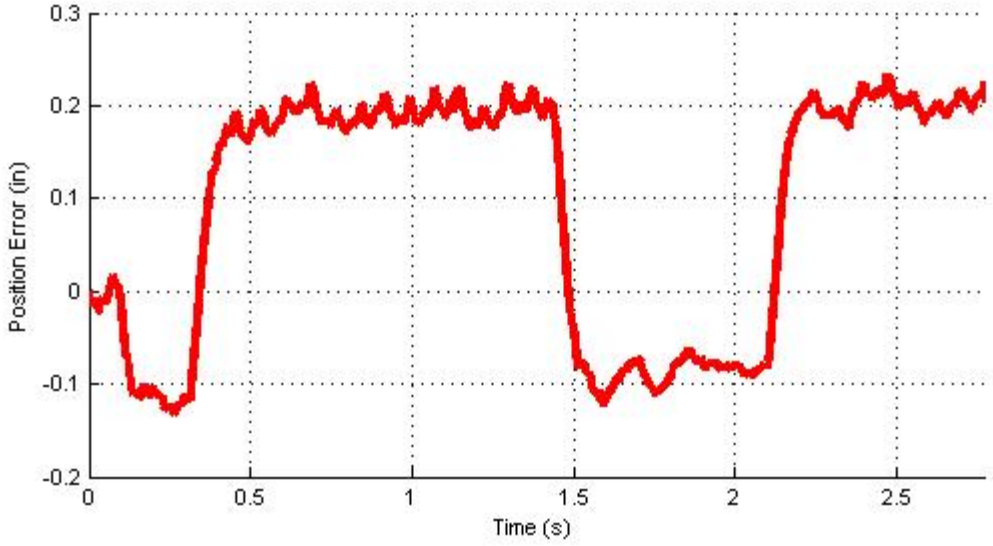

Figure 4-4: Position Error Results of Test #1 (b)

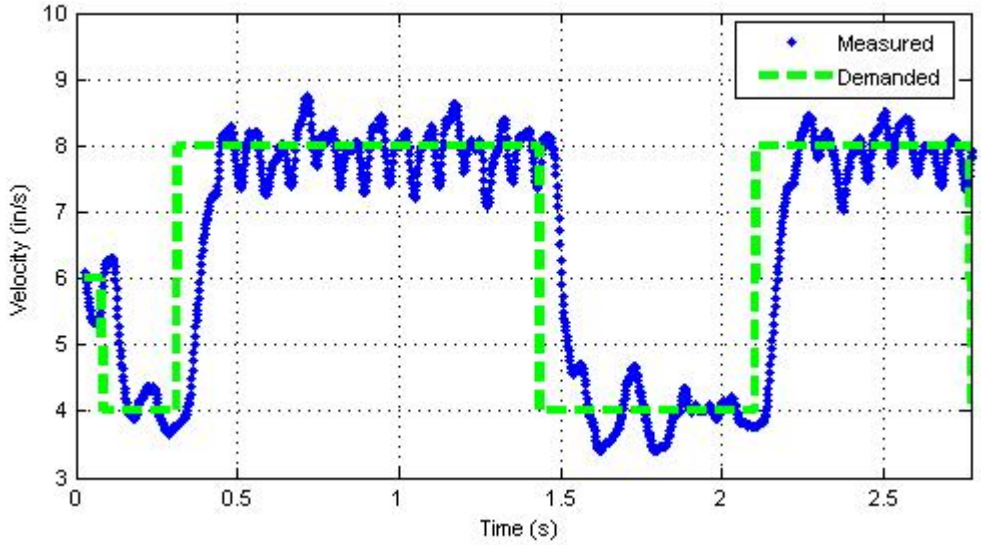

Figure 4-5: Velocity Results of Test #1 (b)

For Test #1 the position error, commanded velocity and measured velocity are plotted over time for objects whose spacing errors were manually entered into the controller. In Case a), the objects were evenly spaced 9 inches apart, and encoder data was recorded from the instant B_1 triggered BS #2. Figure 4-2 shows that object B_2 finishes its buffered trajectory with a position error, indicating the presence of a timing error. The remaining objects end their cycles with the same position error left by B_2,

indicating better performance. Figure 4-3 shows that the actual velocity trajectory resembles the performance expected in Figure 2-8, where each cycle begins with a falling edge of the commanded velocity. For Case b), the objects were spaced randomly. Figure 4-4 and Figure 4-5 show position error and velocity trajectories similar to those of Case a). There is no apparent performance change between handling evenly spaced and randomly spaced objects. As defined in Equation (2-7), the timing error Δt_j for each case is tabulated in Table 4-4.

Table 4-4: Timing Errors from Buffer Regulation of Known Objects

	Test 1 (a)	**Test 1 (b)**
Δt_2 (s)	0.055	0.023
Δt_3 (s)	-0.001	0.003
Δt_4 (s)	-0.016	–

In both cases, the timing error $\Delta t_2 > 0$. This is consistent with the prediction that can be explained as follows: When object B_1 crossed BS #2, it was moving at $\bar{v}$ instead of v_h. This necessitated that B_2 start its buffering cycle at $\bar{v}$ then decelerate to v_l. During the first T_r seconds of the cycle, B_2 did not gain as much distance as if it had started at v_h. At t_s, it will accelerate the full amount, causing a mismatch between the distance gained after t_l and the distance lost after t_s. If B_2 is still behind the nominal trajectory after reaching v_h, it is expected that it will take extra time to reach BS #2. Because the other objects start their cycles with a full velocity change, their delivery times should be much closer to T, which is supported by the results.

For Test #2, the timing errors for both cases are tabulated in Table 4-5

Table 4-5: Timing Errors from Buffer Regulation of Objects with Unknown Spacing

	Footballs					Blocks		
I	Δt_2 (s)	Δt_3 (s)	Δt_4 (s)	Δt_5 (s)	Δt_6 (s)	Δt_2 (s)	Δt_3 (s)	Δt_4 (s)
1	0.002	0.051	-0.029	0.021	-0.003	-0.014	-0.004	-0.012
2	0.015	0.010	-0.001	0.040	-0.040	-0.023	-0.007	-0.012
3	0.039	0.015	-0.002	-0.009	0.011	-0.022	-0.008	-0.022
4	0.001	-0.017	0.001	-0.002	0.004	-0.015	-0.033	-0.012
5	-0.008	0.008	-0.007	0.016	-0.003	-0.022	-0.020	-0.002
6	0.002	0.051	-0.029	0.021	-0.003	–	–	–
				$\bar{\varepsilon}_{\Delta t_j}$				
Average			0.0142				0.0155	
Std. Dev			0.0145				0.0084	

For an average timing error $\bar{\varepsilon}_{\Delta t_j}$ defined by

$$\bar{\varepsilon}_{\Delta t_j} = \frac{1}{IN}\sum_{i=1}^{I}\sum_{j=2}^{N}\left|\Delta t_j\right| \tag{4-4}$$

Table 4-5 shows that both types of objects were delivered with similar average timing errors, but that the balls had a larger standard deviation. Both types of objects were usually delivered with a timing error less than $1/40$ of a second. It is expected that such a timing error would correspond to a tracking error of 0.9 inches, calculated from Equation (2-30). This tracking error is one half of the tracking error expected from the system's average measurement errors. These results indicate that the measurement error does not negatively impact delivery as much as previously thought.

4.4. Two-Conveyor Buffering Regulator Performance

A test of the buffer regulator has been conducted to evaluate its performance when implemented onto a two conveyor system. It is desired to know how timing errors change if the 2nd conveyor is added to the system and whether the placement of BS #1 affects delivery. The remainder of testing done on the buffer regulation algorithm was performed with footballs. Six unique balls were labeled and stuffed with extra mass to simulate the size and weight of typical birds. For this experiment, the footballs were

arranged end to end on the loading conveyor in the same order for each test. Care was taken to ensure that there were small variations in initial spacing such that each iteration was unique.

The hypothesis is that by increasing x_0, there is more time for object B_j to settle upon arrival before l_j and ΔS_j are measured and less time for it to move once measured. If B_j remains stationary on the conveyor surface during and after position detection, measurement errors are reduced and the system delivers it more accurately.

The experiment was performed for two different cases. In both cases, buffer regulation was performed on N = 6 balls with the conveyor speeds matching the parameters of Table 3-6, and the mean initial spacing of objects set to ensure there was no percent mismatch as defined in Equation (3-3). The initial mean spacing S_1 was set at 7.5 in and BS #2 was located at x_f = 100 in. For each iteration, the length and timing error of every ball were recorded. The parameters for the two cases are tabulated in Table 4-6, and the results are shown in Figure 4-6. Additional results are tabulated in Tables A-1 and A-2 for Case #1 and Tables A-3 and A-4 for Case #2.

Table 4-6: Experimental Parameters for Two-Conveyor System

Case #	**I**	$\mathbf{x_0}$ (in)	$\bar{\varepsilon}_{\Delta t_j}$ (s)	
			Average	Std. Dev
1	6	10	0.056	0.051
2	25	30	0.024	0.016

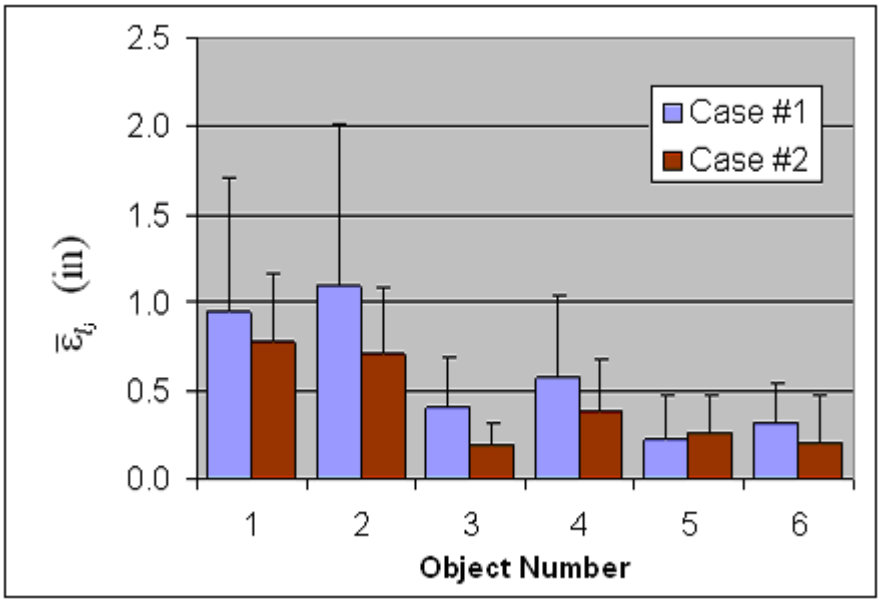

Figure 4-6: Measurement Errors for Two Locations of BS #1

In Case #1, BS #1 was located relatively close to the output of the 1st conveyor, thus allowing a larger $x_f - x_0$. In Case #2, it was much further away, and thus a smaller $x_f - x_0$. The measurement errors, as calculated from Equation (4-1), are plotted against the object number j. Figure 4-6 shows that in nearly every instance, the length is measured more accurately for the conditions of Case #2. It was observed that the balls require a finite amount of time to settle after arriving on the 2nd conveyor due to the velocity change from v_1 to $v_2(t)$. The results indicate that BS #1 should be far enough from the start of the 2nd conveyor that the objects can settle, reducing measurement errors. Table 4-6 shows the average timing error over all iterations for both cases. On average, objects measured under the conditions of Case #1 had roughly three times as large a timing error as those for Case #2. As expected, the larger measurement errors resulted in larger timing errors. Comparing Table 4-5 to 4-6, it can be seen that the two-conveyor system delivers footballs almost as accurately as the single-conveyor system, provided that objects have a chance to settle before position detection. Tables 4-5 and A-4 show the average timing error for the single-conveyor system and for Case #2 to be

0.0142 and 0.0239 s respectively. It is expected that this increase in timing error will result in an extra ⅓ in. tracking error, calculated from Equation (2-30).

4.5. Three-Conveyor Buffering Regulator Performance

A final experiment is conducted to evaluate the performance of the buffer regulator on a three-conveyor system. It is desired to know how the initial spacing on the 1st conveyor affects the tracking error on the 3rd conveyor. A procedure similar to that of the previous experiment was used, wherein N = 5 footballs were loaded on the 1st conveyor, their spacing deviation was measured through position detection, and they were delivered to the end of the 2nd conveyor via buffer regulation using the speeds given in Table 3-6. In this experiment, a 3rd conveyor operated to provide a landing pallet for each object. B_1 moved at a constant speed over the entire length of the 2nd conveyor, so it spent a fixed time traveling from x_0 to x_f = 109 in. (the terminal point of the singulating conveyor). The 3rd conveyor began moving at $t_{0,1}$, with initial conditions such that the first pallet reached x_f at time $t_{f,1}$ in order to meet B_j. Objects directly transferred between conveyors, with $\tau_1 = \tau_2 = 0$.

This experiment was performed for two different cases. Case #1 was a control test, in which the initial spacing was fixed and no buffer regulation was used. Instead, $v_2(t)$ operated at $\bar{v}_2$, and any initial spacing deviations could propagate freely. In Case #2, the controller used buffer regulation to correct for improper spacing. The parameters for these cases are tabulated in Table 4-7:

Table 4-7: Experimental Parameters for Two-Conveyor System

Case #	I	τ_1	Initial Spacing
1	5	0	[10.5, 10.3, 10.4, 10.4]
2	11	0	8 to 14

For this test, balls were placed at a variety of initial spacing types, including end-to-end, clustered, apart and random, and $S_1 + \delta S_j$ was measured before each run. BS #1

recorded the spacing of objects on the singulating conveyor, and a camera near the arrival point of the separating conveyor recorded landing images from which the tracking error could be measured. The tracking error is the signal defined in Figure 2-1 and shown for typical result in Figure 4-7.

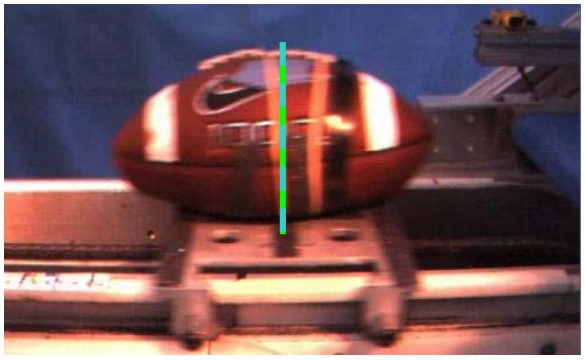

(a) Perfect Delivery

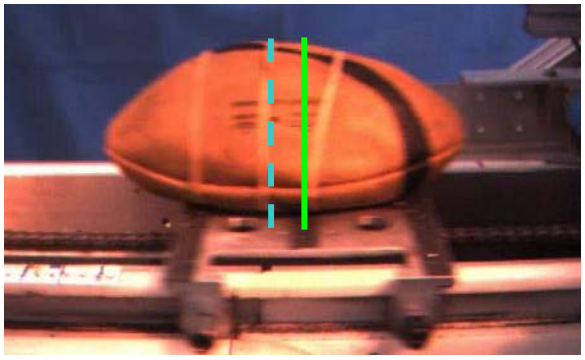

(b) Small Tracking Error

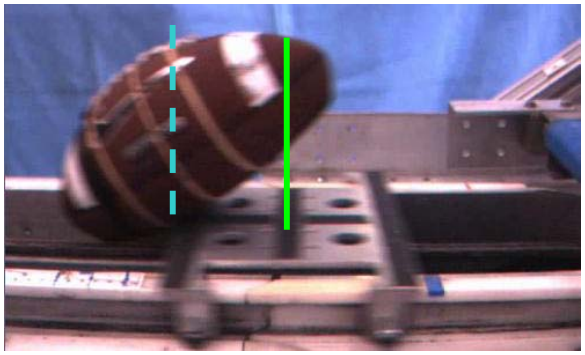

(c) Partial Delivery Failure

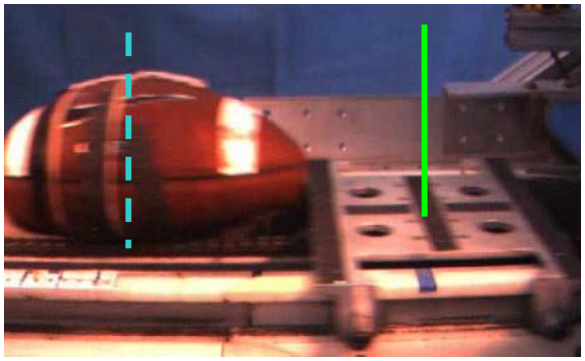

(d) Complete Delivery Failure

Figure 4-7: Tracking Error of Typical Delivery Results

In Figure 4-7, the motion of the system is right to left; the dashed line represents x_j and the solid line represents p_j. In (a), the desired result is shown: a perfect delivery with zero tracking error. In (b), the ball is ahead of the pallet by a small amount, yielding a positive tracking error. If the ball was misplaced by only a few inches, it usually fell off the pallet, resulting in a partial delivery failure, as shown in (c). Any more than that and the ball will miss the pallet entirely, resulting in a complete delivery failure, as shown in (d). Because the pallets are spaced to match the conveyor's constant speed, delivery onto the pallets will ensure the throughput requirement is met.

The initial spacing, spacing deviation, landing condition and tracking error for all iterations are tabulated in Appendix A. Table A- 5 contains the results of Case #1, Table A-6 and A-7 contains the results of Case #2. For the conditions of Case #2, 35 additional iterations were performed, only recording the initial spacing and tracking error for each ball. These results are tabulated in Table A- 8. The primary results from this experiment are shown below in Figure 4-8.

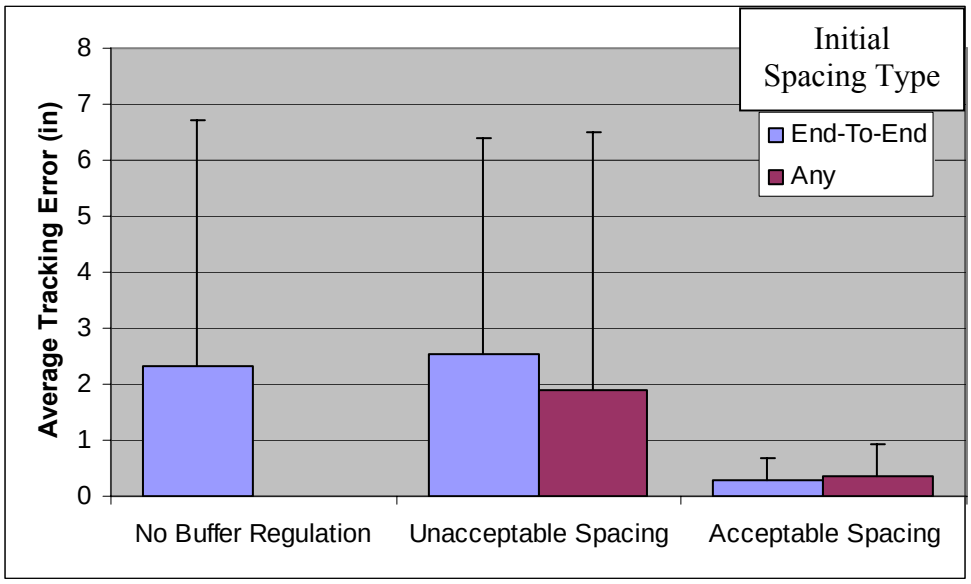

Figure 4-8: Average Tracking Errors of Objects on a Three-Conveyor System

The average tracking error is compared for both cases and for different spacing deviations and initial spacing types. Acceptable spacing is defined for an instance in which ΔS_j was inside the acceptable bounds of Table 3-10 for all five footballs. Unacceptable spacing occurs when at least one ball was outside that range. Figure 4-8 shows that, as expected, the control test produced very large tracking errors. Often for Case #1, B_2 would be delivered at the edge of the pallet, B_3 would be a partial delivery failure, and B_4 and B_5 would be complete delivery failures. For Cases #2, in which buffer regulation was used, there was not a single partial or complete failure, provided that spacing was acceptable. Figure 4-8 shows that when ΔS_j had unacceptable spacing, the system performed about as well as if there were no buffer regulation at all.

Because the spacing deviations on the 2nd conveyor play such a large role in determining the final tracking error, it is important to understand the correlation between the spacing of objects on the 1st and 2nd conveyors. To this end, the initial spacing is plotted against the spacing measured for objects as they passed through BS #1 on the singulating conveyor.

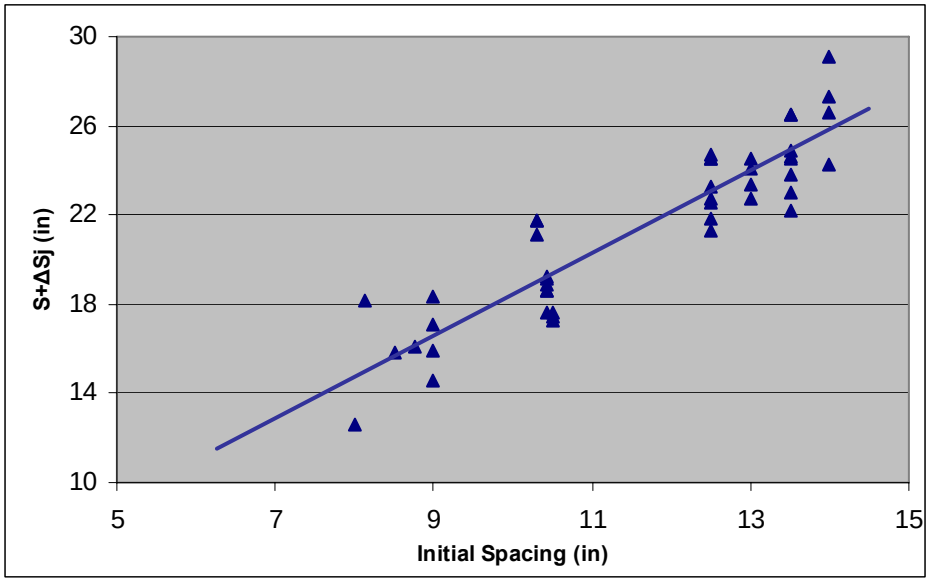

Figure 4-9: Correlation between Spacing on 1st and 2nd Conveyors

Figure 4-9 shows that the spacing on the 2nd conveyor is directly proportional to the spacing on the 1st conveyor. A least squares line fit to the data yields an 83% correlation between the initial and intermediate spacing. This result indicates that the acceptable spacing bounds on the 2nd conveyor correlate to acceptable spacing bounds on the 1st conveyor.

The results in Tables A-6 through A-8 show that when balls were initially spaced between 9.5 and 13 inches on the loading conveyor, the buffer regulator delivered them with minimal tracking error. From this result, the nominal initial spacing S_1 is set as the midpoint of this range, 11.25 in. If the balls were initially spaced too far away from S_1, ΔS_j exceeded the tolerable spacing bounds and large tracking errors occurred. For object B_j initially spaced at $S_1 + \delta S_j$, the absolute initial spacing deviation is $\left|\delta S_j\right|$.

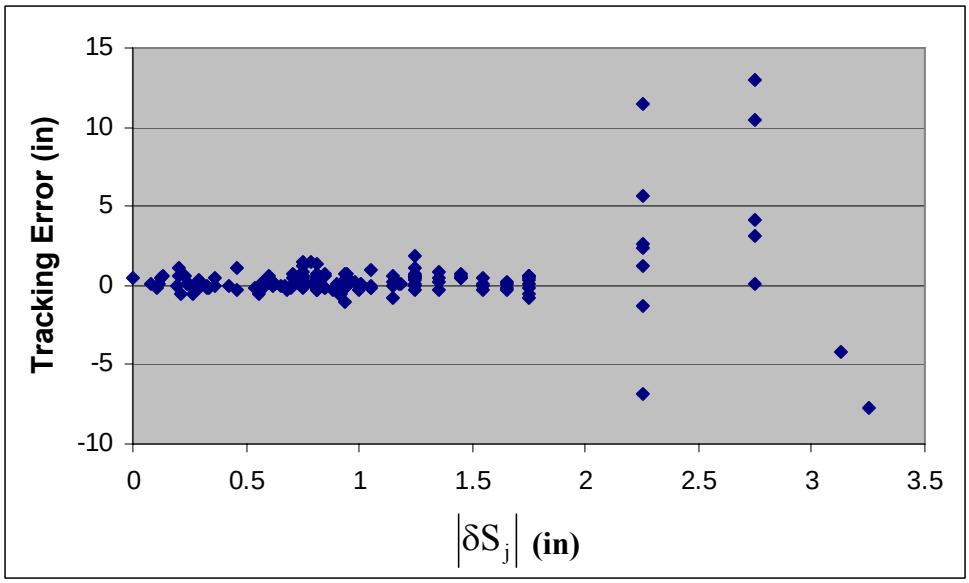

Figure 4-10: Initial Spacing and Tracking Error

The absolute initial spacing deviations are plotted against the resulting tracking error for all iterations under the conditions of Case #2. Figure 4-10 demonstrates the tracking error disparity between small and large initial spacing deviations. Of 164 balls with $|\delta S_j| < 2$ in., not a single one exhibited either type of delivery failure. If instead the balls were placed outside of that range, their tracking error was usually large enough to create partial and complete delivery failures.

The results of this final experiment show that the buffer regulation algorithm is very effective at accurately delivering balls provided that the initial spacing deviations are small. To quantify the efficacy of the regulator, the initial spacing variation is compared to the final spacing. The average initial spacing variation $\delta\bar{S}$ is defined in (4-5),

$$\delta\bar{S} = \frac{1}{IN}\sum_{i=1}^{I}\sum_{j=2}^{N}|\delta S_j| \qquad \textbf{(4-5)}$$

Because the pallets are equally spaced, the average final spacing deviation is equivalent to the average tracking error $\bar{e}$. These average spacings can be normalized dividing by the mean spacing for its respective conveyor. The normalized average spacing are $\delta\bar{S}/S_1$

and $\bar{e}/S_3$ for the initial and final conveyors respectively. For instances of Case #2 where $\left|\delta S_j\right| < 2$ in., Table 4-8 tabulates the change of average spacing deviations.

Table 4-8: Initial vs Final Spacing Deviation

	Average (in)	Standard Deviation (in)	Normalized Average -	Standard Deviation -
$\delta\bar{S}$	0.891	0.400	0.0792	0.0356
$\bar{e}$	0.206	0.430	0.0057	0.0119
Improvement Ratio	**4.3:1**	**0.93:1**	**13.8:1**	**3.0:1**

Table 4-8 shows that the buffer regulator significantly reduced the spacing variation over the course of the system to accurately deliver randomly-spaced objects. For footballs arriving with small initial variations, the average tracking error produced was 0.21 in.

4.6. Summary

In this chapter, the effects of the buffer regulation algorithm were experimentally investigated. The algorithm developed in Chapter 3 was found to be very effective at measuring and delivering objects on a single-conveyor system. When expanded to a two-conveyor system, the system performed nearly as well. For a complete three-conveyor system, the buffering regulator was found to successfully deliver objects on the pallets with an average tracking error of 0.2 inches, reducing the normalized spacing deviation by a factor of nearly 14 over the course of the system. The results from the experiments confirmed the predictions of the simulations. Namely, the initial spacing of the objects must correspond to the demanded throughput and allow for tolerable spacing deviations on the singulating conveyor.

CHAPTER 5

CONSIDERATION OF PRACTICAL IMPLEMNTATION

5.1. Introduction

In the previous Chapter the implementation of buffer regulation proved very successful at accurately delivering randomly-spaced inanimate objects of simple shape, provided that they transfer directly between conveyors. This chapter discusses issues regarding practical implementation of the buffer regulation algorithm to a more complex system. Considered are systems that may contain extra transfer mechanisms or must process live objects. A method of detecting irregular objects is proposed and experiments are conducted to asses its performance.

5.2. Effects of Additional Variability

The experiments performed in Chapter 4 were designed to transfer objects directly between conveyors such that $\tau_1 = \tau_2 = 0$. In a typical production line, this may not be the case. Depending on the size of the conveyors, the shape of the objects or the layout of the processing facility, additional mechanisms may be required for object transfer, adding time delays into the operation of the buffer regulator. Such a mechanism may not operate in a uniform manner for each object, randomly affecting the spacing deviation. For this section, an experiment was conducted to examine the effects when extra variability is introduced into the system.

The experiment was conducted with the same setup and parameters used in Section 4.5 but with one key change: a singulator, comprised of a pair of counter-rotating drums, bridged the gap between the loading and singulating conveyors. The drums contained a series of flexible fingers that adjusted to the size of the footballs and provided

enough support to transfer them securely. The singulator also worked to orient the footballs during transit, delivering them aligned with the direction of motion. For an application involving live birds, a singulator is often necessary to separate clustered birds and align them single file to be processed one at a time. When properly operated in conjunction with a conveyor, the singulator can be used to help regulate spacing deviations and keep birds stable across conveyor gaps.

It is not the focus of this thesis to examine the nominal operating parameters for the singulator. Instead, it will only be used to introduce extra variability into the system to asses the robustness of the buffer regulation algorithm. As footballs passed through the drums, the singulator took a random time $\tau_1 \neq 0$ to transfer them onto the singulating conveyor. The parameters for this experiment are tabulated in Table 5-1 and the results are tabulated in Tables B.3 and B.4.

Table 5-1: Initial vs Final Spacing Deviation

Parameter	Value
I	16
Initial Spacing (in)	7 to 13.5

The results indicate that extra variability significantly reduces the performance of the system. Even though the footballs were loaded with initial spacings similar to those used in the three-conveyor test of Chapter 4, fewer were delivered to the pallets with the same accuracy. Notably, the correlation between the initial spacing and the spacing on the 2nd conveyor has been reduced, as shown in Figure 5-1.

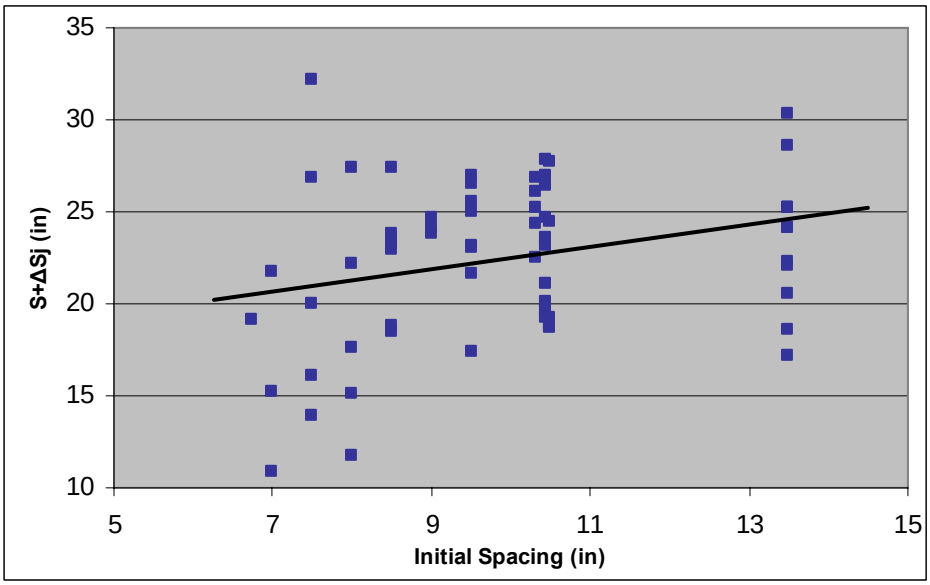

Figure 5-1: Correlation between Spacing on 1st and 2nd Conveyors

The spacing on the 2nd conveyor is plotted against that on the 1st for each ball and a least squares line is fit to the results. When extra variability is introduced, the correlation dropped to 8.1% (down from 83% shown in Figure 4-9). As a result, many fewer iterations resulted in appropriate spacing deviations. Even if balls had small initial spacing deviations, they were not assured proper delivery. Figure 5-2 shows the delivery results for instances when $\left|\delta S_j\right| < 2$ in.

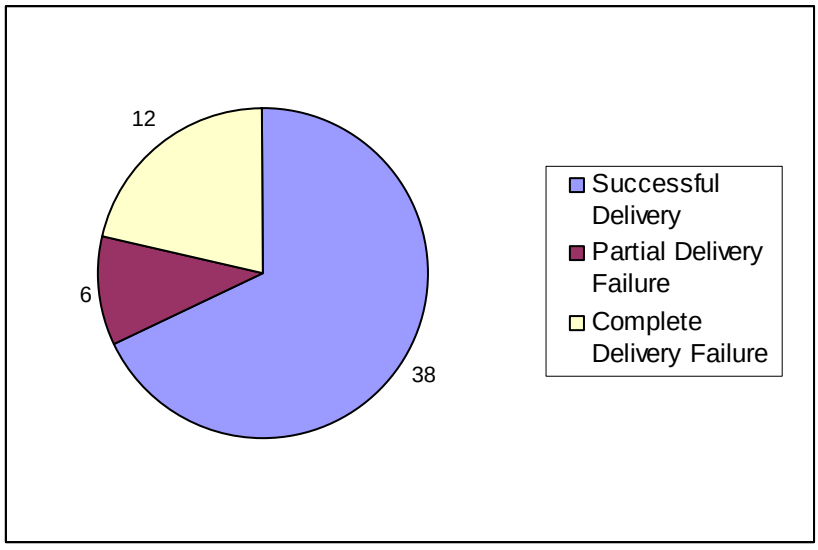

Figure 5-2: Number of Balls Delivered for All Delivery Types when Singulated

Figure 5-2 indicates that the initial spacing range which guaranteed successful delivery when $\tau_1 = 0$, did not guarantee success when $\tau_1 \neq 0$. There may exist a constant $\left|\delta S_j\right| < c < 2$ in. for which singulated objects could have been properly delivered. However, Figure 5-1 suggests that there is practically no correlation between initial spacing and ΔS_j. If the extra variability caused even perfectly-spaced objects to be delivered to the 2nd conveyor with ΔS_j outside of the acceptable range, it is unlikely that any value of c could guarantee success under the experimental operating parameters.

Instead, we consider what operating parameters could have accommodated the spacing range produced by the addition of extra variability. It was found that for cases in which the balls were loaded with $\left|\delta S_j\right| < 2$ in. the maximum and minimum spacings produced on the 2nd conveyor were 27.83 and 17.35 in. respectively. For the same T and T_u, the speeds v_h and v_l must change to create spacing bounds equal to or greater than these values. To do so, the desired bounds are substituted into Equation (2-17) to create a system of equations shown in Equation (5-1).

$$\frac{1}{2}\begin{bmatrix}(2T - T_u) & T_u \\ T_u & (2T - T_u)\end{bmatrix}\begin{bmatrix}v_h \\ v_u\end{bmatrix} = \begin{bmatrix}S + \Delta S_j \\ S - \Delta S_j\end{bmatrix} \quad \textbf{(5-1)}$$

For the spacing bounds produced using extra variability, Equation (5-1) becomes Equation (5-2).

$$\begin{bmatrix}1.152 & 0.181 \\ 0.181 & 1.152\end{bmatrix}\begin{bmatrix}v_h \\ v_u\end{bmatrix} = \begin{bmatrix}27.83 \\ 17.35\end{bmatrix} \quad \textbf{(5-2)}$$

The solution to Equation (5-2) is tabulated in Table 5-2, along with the bounds and speeds for the system without the singulator, and for a hypothetical case in which objects could be delivered onto the singulating conveyor with spacing deviation equal to the length of an average bird.

Table 5-2: Required Conveyor Speeds for Various Spacing Deviations

	Selected	No Additional Variation	With Additional Variation	Hypothetical Bird Spacing
$\mathbf{S+\Delta S_j}$ (in)	25.22	24.67	27.83	28.89
$\mathbf{S+\Delta S_j}$ (in)	17.45	17.66	17.35	13.77
$\mathbf{v_h}$ (in/s)	20	20	22.34	23.78
$\mathbf{v_l}$ (in/s)	12	12	11.55	8.22

In Table 5-2, the selected values are those chosen in Table 3-6 and calculated in Table 3-10. For the values shown without additional variations, the bounds are taken from Table A- 6 and the speeds are those used for the respective experiment. For the values with additional variation, the speeds are the solution to Equation (5-2). The speeds for the theoretical case are calculated from Equation (5-1) for the spacing bounds listed. Table 5-2 indicates that to accommodate the variability introduced by the singulator, the velocity range would have to increase by roughly 35% from the original parameters. To accommodate object B_j arriving with ΔS_j equivalent to the length of a bird, the velocity range must almost double from the original parameters.

If the 2nd conveyor is limited by a saturation velocity of 20 in/s, the experimental system can not accommodate much additional variability. However, by increasing the velocity limit only 4 in/s, the system can be designed to process objects arriving with spacing deviations twice as large, and thus much more variability. However, it should be noted that the conveyor speeds can impact the spacing deviations. Increasing the velocity range could magnify the effects of additional variation, still producing objects outside of the increased spacing range. Additionally, it was discussed in Chapter 3 that as the velocity range increases, it becomes more difficult to ensure that objects do not move relative to conveyors, especially for live objects. For these reasons, before implementing different parameters, further testing should be conducted to determine the effects of the velocity range upon object reactions and spacing. Nonetheless, the results indicate that

the buffering regulator does contain the ability to account for additional random variations in spacing.

5.3. Effects of Irregular Objects

The position detection described in previous chapters relies on two assumptions about the objects being processed. First, the objects have a well defined shape. Second, they are oriented so they can be detected by a simple point proximity beamswitch. In an application to process birds, these criteria will not be met. In this section, we examine an alternative method using a column of multiple beamswitches.

Consider an object such as a bird that has a primary body with relatively small secondary appendages protruding from it. In order to locate the center of the primary body, the sensor must ignore the appendages. This feat can be performed with a vertical column of beamswitches, which together output a signal only when a contiguous number of beams of height d are broken. The value of d need only be large enough to encompass the maximum cross-sectional height of the largest tolerable appendage. If d is less than this value, the beamswitch array could mistake a secondary object as part of the primary one, significantly affecting the center calculation. If d is much greater than the appendage height, significant portions of the body would fail to trigger the beamswitch. The desired effect is shown below in Figure 5-3.

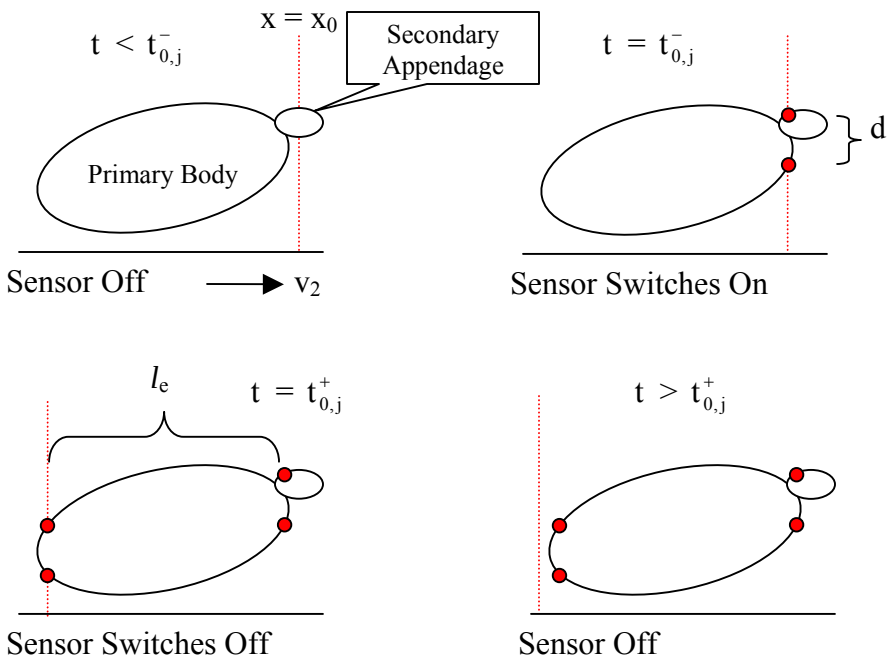

Figure 5-3: Side View of Irregular Object Passing Through Column of Beamswitches

The red dots in Figure 5-3 indicate the location on the object at which the sensor signal would change. The large ellipse represents the body, while the smaller one represents an appendage, such as a head. Note that this appendage has a height less than d. Because the front tip of the body also has a height less than d, it too may be ignored. A similar, though not necessarily equal, length could be ignored from the rear of the object. The two ignored lengths might be different for the object pictured above because of the location of the appendage or the shape of the body. The difference between the start and end of the sensor trigger yields an effective length, l_e, which by definition is less than or equal to l, the actual length of the object's body.

To process the object through buffer detection, knowing the center of the object is more important than its effective length. However, because the effective length affects the center calculation, accuracy in both values is desired. If an equal amount of the front and back of the body is ignored, the calculated center should exactly match the actual center, regardless of the discrepancy between l_e and the actual object length.

Implementation of this technique into the buffer regulation algorithm will change some of the key parameters. Most notably, the time required to perform a sensor scan will increase, as T_{bs} is proportional to the number of sensors used.

Experimental Setup

To meet the specifications of this method, Banner A-GAGE® MINI-ARRAYS® were used. These beamswitches consist of two columns of photoelectric sensors mounted vertically, as shown in Figure 5-4. The path of each beam traversed the width of the singulating conveyor, and the beamswitches were tall enough so that birds in any orientation could not rise above the highest sensor. Accurate bird detection required the use of 30 sensors per beamswitch. The maximum scan time required increased to 3.26 ms [Banner]. With all other systems identical, the new unusable time per cycle will increase to 323.02 ms.

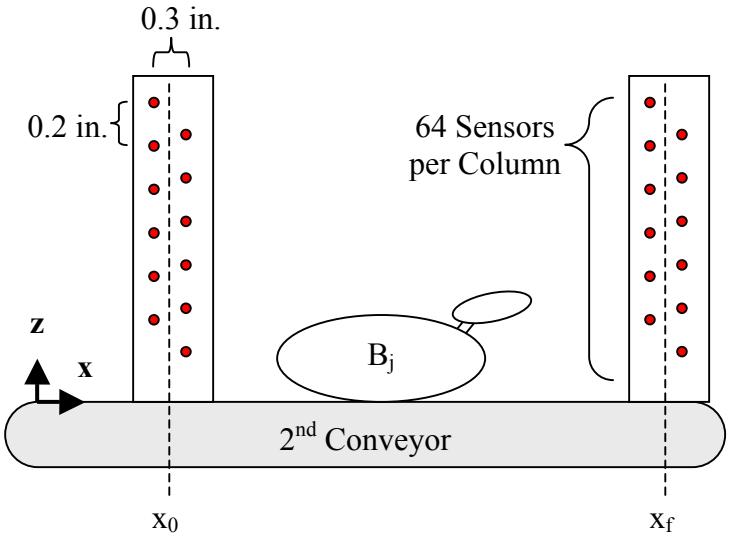

Figure 5-4: Side View of Experimental Setup using Multi-sensor Beamswitches

The position detection routine is changed slightly to accommodate multiple sensors. For two columns of sensors, $t_{0,j}^{-}$ will occur when the front of B_j triggers the first column and $t_{0,j}^{+}$ will occur when the rear of B_j clears the second column. If both sensor

columns are used to calculate l_j, Equation (2-25) is changed to include the distance between columns shown in Figure 5-4. The new calculation is performed with Equation (5-3).

$$l_j = \int_{t_{0,j}^-}^{t_{0,j}^+} v_2(t)dt - 0.3 \text{ in.} \quad \textbf{(5-3)}$$

Now, the object need not be completely symmetric to be located, provided that its center still lays in the middle of a symmetric primary shape.

Effects of Irregular Objects on Position Detection

Two experiments were conducted to evaluate the performance of the position detection routine. In the first experiment, it was desired to determine what value of d should be used to properly ignore the length contributions of secondary appendages on bird-like objects.

In Lee [2001], 120 chickens were weighed and measured. 57 of the birds were female, and all were typical of those used in poultry processing plants. It was found that a bird torso could be modeled as an ellipsoid, a shape that has a very simple geometric center. The key measurements from that study are presented in Table 5-3.

Table 5-3: Chicken Torso Measurements

	Unit	Mean	Std. dev.
Weight	(kg)	1.67	0.15
Height	(mm)	113	11
Length/Height		1.7	0.2

From the perspective of the beamswitch, the average chicken torso should appear as an ellipse with a height of 113 mm (4.45 in) and a length of 192 mm (7.56 in.). From observations, it can be noted that sitting chickens rest at a relatively low angle with respect to the conveyor surface. Even if this were not the case, an ellipse is rotationally symmetric, so the center of an inclined bird would match that of the same bird resting flat. An object is built based on the findings of this study, as shown below in Figure 5-5.

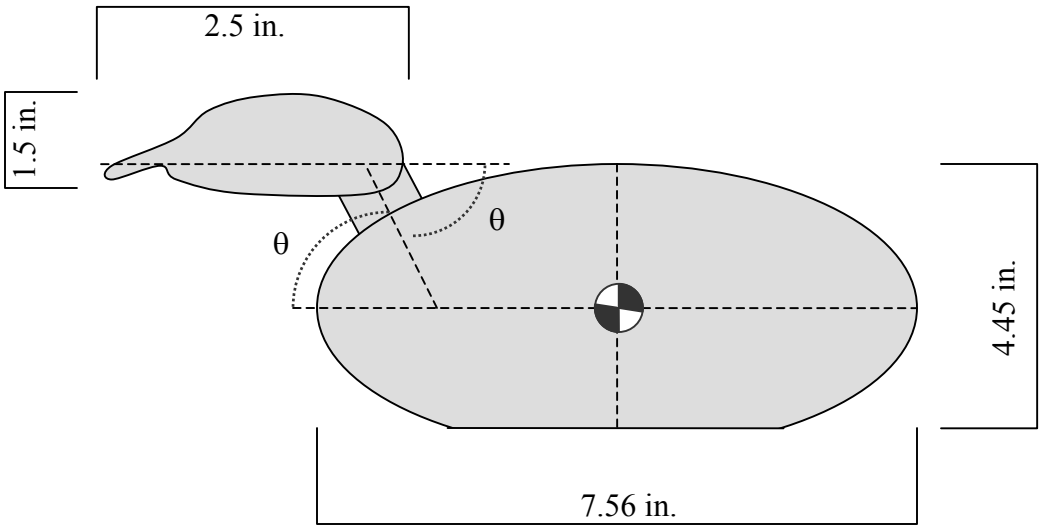

Figure 5-5: Model Bird

The model contained a head and neck that pivoted about a point on the principle axis. The head was always pointed forward, but the neck could be set at any angle θ between 0 and 90^{o}, with zero being straight forward and ninety being straight up. Because of irregularities caused by the inclusion of a head and neck, such an object could not be accurately measured with just a single-point beamswitch.

For the first experiment, BS #1 was configured as a scanner, sampling its sensors every tenth of a second and outputting the image. The model was placed on the singulating conveyor, which operated at 1 in/s. As the model crossed BS #1, an image was generated of its profile. This occurred for five iterations, with θ set at 0, 30, 45, 60 and 90 degrees respectively. Figure 5-6 through Figure 5-10 show the generated images for each configuration.

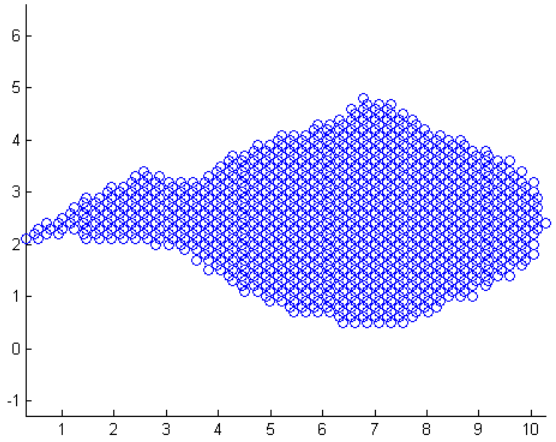

Figure 5-6: Scanned Image of Model Bird with 0^{o} Neck Angle

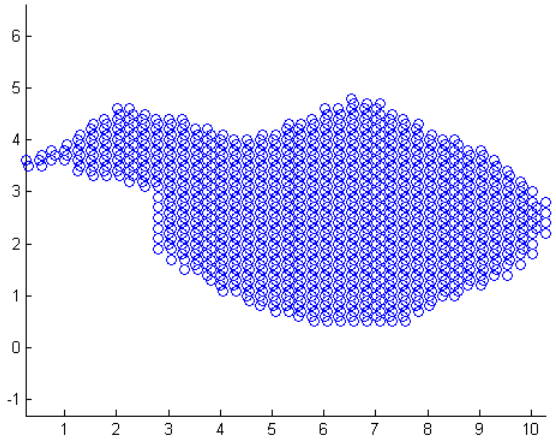

Figure 5-7: Scanned Image of Model Bird with 30^{o} Neck Angle

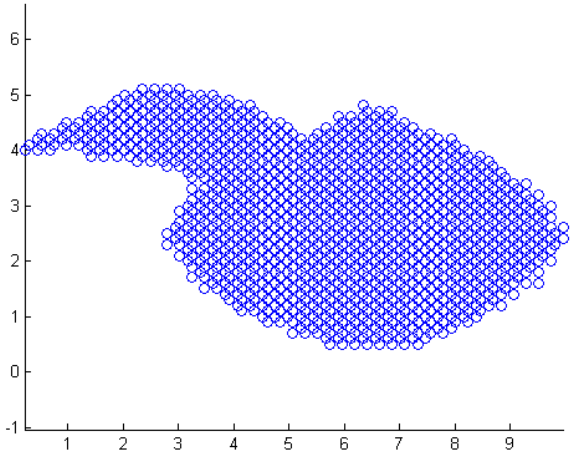

Figure 5-8: Scanned Image of Model Bird with 45^{o} Neck Angle

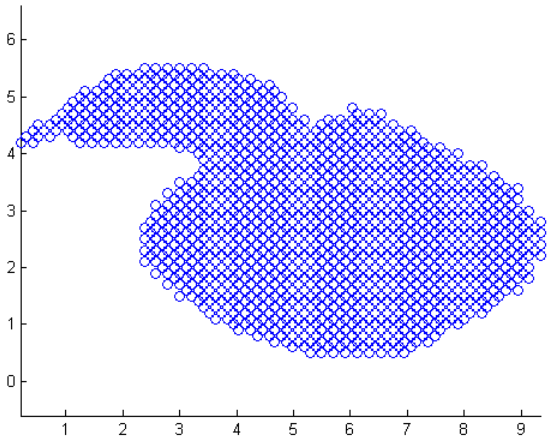

Figure 5-9: Scanned Image of Model Bird with 60^{o} Neck Angle

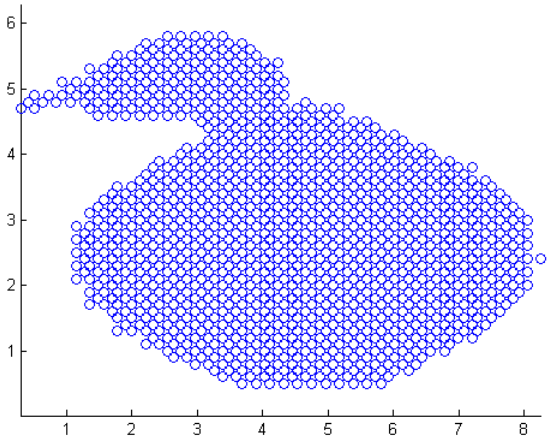

Figure 5-10: Scanned Image of Model Bird with 90^{o} Neck Angle

Analysis of the images concluded that $d \geq 1.6$ in. in order for the beamswitch to ignore the head. If both sensor columns are used for position detection, this value corresponds to a minimum of 16 blocked beams. If only one column is used, 9 beams must be blocked to change the beamswitch signal. These values were verified by configuring the beamswitches as stated and putting the model's head across the beams. No neck orientation caused the beamswitch to trigger. However, when the configurations were reduced to 15 beams for two columns and 8 beams for one, the beamswitch would trigger for the head at various neck angles.

The second experiment tested how the two configurations impacted the length and spacing measurement errors. The model bird was mounted 11.21 in. away from a rod of uniform width. The two objects were placed on the singulating conveyor, which operated at v_l to move them through BS #1. Using position detection, the length and spacing of the model was recorded for 15 iterations of each configuration (1 column, 2 columns) and neck angle (θ = 0, 30, 45, 60, 90^o). The results are tabulated in Tables B-1 and B-2 and plotted in Figures 5-11 and 5-12.

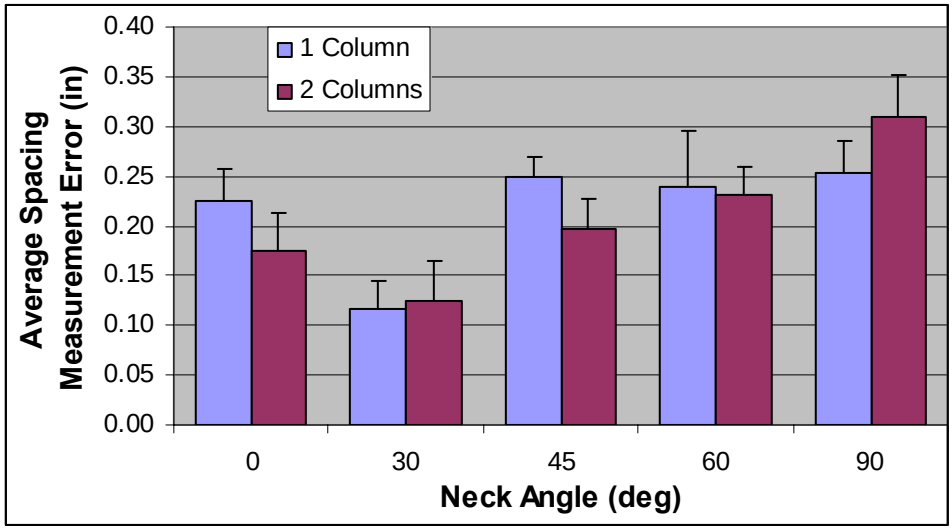

Figure 5-11: Spacing Error of Model Bird

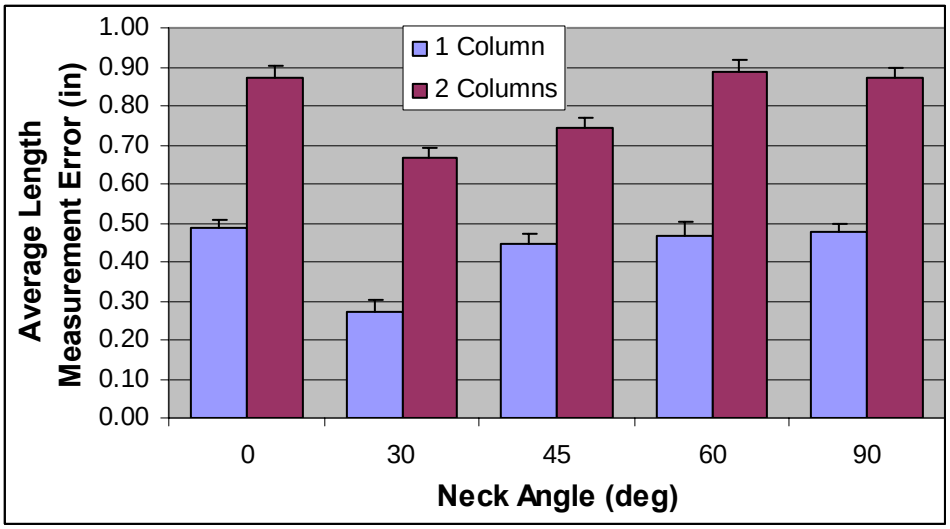

Figure 5-12: Length Error of Model Bird

For spacing measurement errors, there was no significant difference between using one column of sensors or both. For the length, however, the errors for using one column were about half those for using two. The average length and spacing measurement errors were lower at a neck angle of 30^o than for other angles, but there seemed to be no general correlation between neck angle and measurement error. When using one column of sensors, the average spacing measurement error over all neck angles was 0.22 in. For a bird roughly 10 inches from beak to tail, locating the center of its torso to within a quarter of an inch is quite accurate. For comparison, the position detection routine could measure ΔS_j between well defined objects with a measurement error of about 0.1 in., yielding an average tracking error of 0.21 in. when the spacing was within tolerance. From Equation (2-28), this increase in error should result in an additional 0.01 s of timing error, producing a tracking error that increases by 0.27 in from Equation (2-30). For a final average tracking error of 0.48 in, the objects should still land cleanly on the pallet.

5.4. Summary

In this chapter two experiments were conducted to address practical implementation of the buffer regulation algorithm. It was found in the first experiment that the system performance is reduced for systems with additional transfer mechanisms that introduce additional spacing variation. For the second experiment, a method to locate the center of irregular objects was proposed. It was found that implementation of the method could accurately locate the center of a bird shaped object to within a quarter of an inch.

CHAPTER 6

SUMMARY AND FUTURE WORK

This chapter summarizes the contributions made in this thesis and highlights the remaining work to be done.

6.1. Summary

The use of a switching controller has been proposed to create a buffer regulator for the delivery of randomly spaced objects across three serially-connected conveyors according to a demanded spacing and throughput. A formulation has been presented to determine the nominal operating conditions and stability based on the system parameters. The buffering regulator has been implemented with an algorithm to detect the length and spacing of objects on a conveyor, which requires only an encoder and two beamswitch inputs for calculation of the switch time necessary for proper delivery.

The performance of the algorithm has been tested experimentally. It consists of two routines: a position detection routine to locate objects and a buffer regulation routine to adjust the conveyor velocity accordingly. The position detection routine has been tested with engineering objects and found to accurately measure the length and spacing. Position detection was also found to be more accurate when the required sensor is located far enough away from conveyor transitions to allow objects to settle. The buffer regulation routine has been tested and found to be effective at delivering the same objects with minimal timing errors for a limited range of spacing deviations.

Design considerations have been discussed for choosing the nominal operating parameters. Operating conditions have been shown to impact the amount of variation the

system can handle, the quantity of measurement errors and the effect those errors have on system performance. Based on the nominal operating parameters and physical constraints, the spacing limits have been derived within which the algorithm should be able to accurately deliver objects.

The buffering regulation algorithm has been used to simulate the effects of initial variations on object delivery. Through simulation, throughput mismatches between conveyors have been found to negatively impact the stability and performance of the system. Increasing the variability of the initial spacing has also been found to increase the quantity, but not magnitude, of delivery errors. Experimentation has confirmed that increasing the initial variability reduces system performance. Testing has shown that for a system in which initial spacing is the primary source of variability, there exist initial spacing conditions for which successful deliver can be guaranteed. Once those conditions are broken, the effects of the buffering regulation algorithm have been found to be no better than those of a system with no control at all. For the same operating parameters, introduction of additional spacing variability between conveyors has been found to reduce the performance of the system. Necessary changes to the operating parameters to account for extra variability have been proposed.

For an experimental setup with cycle time 4/3 s, input speed 10 in/s, output speed 27 in/s, initial absolute spacing deviation less than 2 in., characteristic conveyor time 0.18 s, and no time delays between conveyors, optimal operating parameters have been determined. Implementation of the buffer regulation algorithm has been found to deliver sets of five footballs onto equally spaced pallets with average tracking error 0.21 inches, reducing the normalized variability of the system by a factor of nearly 14.

To measure the location of irregularly shaped objects, a modified position detection routine has been proposed for use with line scanners. The modified routine used additional sensor information to ignore small appendages protruding from a primary body. Although implementation of the routine for use with inanimate birdlike objects has

been found to measure objects with less accuracy than for simpler objects, the additional measurement error has been found not to significantly reduce system performance.

6.2. Future Works

The buffer regulation algorithm developed in this thesis has proven very effective for delivering a limited range of randomly spaced inanimate objects. To asses how effective the algorithm would be if implemented in a poultry processing plant or another suitable field, further study should be conducted. The following are recommendations of future work that could build upon this thesis:

1. Investigate the efficacy of the algorithm when using live broilers.
2. Investigate the efficacy of the algorithm with large volume tests
3. Modify the velocity profile through trajectory planning to compensate for the known conveyor dynamics. This has the potential to reduce the unusable cycle time and increase the tolerable spacing.
4. Develop a method to monitor the throughputs of each sub-system and adjust the velocities accordingly.
5. Determine the effects of acceleration on object stability to maximize the velocity range.

APPENDIX A

BUFFER REGULATION EXPERIMENTAL RESULTS

An experiment was conducted to investigate the effects of sensor placement on the accuracy of measurements and delivery. For a two-conveyor system, objects transferred from the 1st conveyor to the 2nd, were measured using the position detection routine and delivered via buffer regulation. The position detection beamswitch was placed in two different locations, one close to the conveyor transfer at x_0 = 10 in. and one further away at x_0 = 30 in. The measurement errors and subsequent timing errors are tabulated in Tables A-1 through A-4. For iterations 9 and 20 of Table A.4, timing data was not recorded.

Table A- 1: Length Measurement Errors of Footballs for x_0 = 10 in.

	ε_{l_j} (in)					
Iteration	**j=1**	**2**	**3**	**4**	**5**	**6**
1	0.48	-0.02	0.49	0.05	0.11	0.38
2	-0.59	-1.07	-0.91	-1.23	-0.71	0.32
3	-2.14	-2.09	0.43	-0.32	0.12	0.05
4	0.09	-0.05	0.22	-0.91	-0.15	-0.07
5	-1.59	-1.24	-0.09	-0.16	0.22	0.63
6	0.82	-2.10	0.29	-0.75	0.02	0.47
Average	0.95	1.09	0.40	0.57	0.22	0.32
Std Deviation	0.76	0.92	0.28	0.47	0.25	0.23

Table A- 2: Length Measurement Errors of Footballs for x_0 = 30 in.

	ε_{l_j} (in)					
Iteration	**j=1**	**2**	**3**	**4**	**5**	**6**
1	-1.09	-0.68	-0.25	0.40	0.17	0.06
2	0.76	0.91	-0.18	0.20	0.11	-0.85
3	0.35	0.36	-0.11	-0.85	-0.92	-0.02
4	0.94	0.90	0.23	0.41	-0.36	-0.07
5	0.72	0.15	0.02	0.16	-0.05	-0.32
6	-0.52	-0.51	-0.29	0.67	-0.08	0.05
7	0.90	0.90	-0.26	0.64	-0.34	-0.31

8	0.89	-1.24	0.32	-0.37	0.12	-0.33
9	0.56	0.69	-0.18	0.50	0.15	0.15
10	0.43	0.97	-0.16	0.74	0.24	0.00
11	-0.44	0.28	-0.22	0.09	0.04	0.13
12	-1.28	1.03	0.20	0.41	0.11	0.28
13	0.08	0.58	0.01	-0.87	0.37	0.09
14	0.28	0.63	0.13	-1.00	-0.28	0.06
15	0.68	0.29	-0.04	0.07	0.07	0.16
16	0.65	0.33	-0.20	0.28	0.37	-0.07
17	0.97	-0.49	-0.18	0.21	0.50	-0.13
18	-0.68	0.33	0.52	0.44	-0.10	-0.11
19	1.12	0.79	0.06	0.28	0.11	0.25
20	0.98	0.60	-0.33	0.20	0.25	0.14
21	-1.67	1.01	-0.17	0.63	-0.72	-0.05
22	0.25	0.64	-0.02	-0.01	0.07	0.01
23	-1.61	-1.88	0.12	0.07	0.27	0.26
24	-0.69	0.67	0.14	0.05	-0.13	-1.16
25	0.88	0.86	0.43	-0.04	0.40	0.02
Average	0.95	1.09	0.40	0.57	0.22	0.32
Std. Deviation	0.76	0.92	0.28	0.47	0.25	0.23

Table A- 3: Timing Errors of Footballs for x_0 = 10 in.

	Δt_j (s)				
Iteration	**j=2**	**3**	**4**	**5**	**6**
1	0.023	0.102	0.002	0.059	0.017
2	-0.019	0.072	0.062	0.068	0.001
3	0.072	0.206	0.003	0.067	0.019
4	-0.135	0.118	0.026	-0.026	0.046
5	-0.054	0.147	0.016	0.042	0.000
6	-0.048	0.143	0.033	0.029	-0.016
Average	0.056				
Std Deviation	0.051				

Table A- 4: Timing Errors of Footballs for x_0 = 30 in.

	Δt_j (s)				
Iteration	**j=2**	**3**	**4**	**5**	**6**
1	0.042	0.002	0.037	-0.003	0.048
2	0.023	0.004	0.005	-0.001	-0.018
3	0.027	0.009	0.015	-0.003	-0.011
4	0.030	0.006	-0.006	0.004	-0.008
5	0.043	0.015	-0.003	0.006	0.003
6	0.028	0.031	0.044	0.011	0.019
7	0.028	0.022	0.016	0.027	0.028

8	0.031	0.020	-0.004	0.013	-0.006
9	-	-	-	-	-
10	0.052	0.028	0.020	0.012	0.010
11	0.055	0.013	0.013	0.017	0.016
12	0.066	0.035	0.010	0.015	0.009
13	0.048	0.034	0.034	0.009	0.030
14	0.046	0.035	0.037	0.019	-0.026
15	0.058	0.012	0.050	0.031	0.028
16	0.054	0.042	0.009	0.042	0.022
17	0.045	0.039	-0.001	0.007	0.026
18	0.047	0.035	0.022	0.015	0.006
19	0.039	0.035	0.036	0.002	0.014
20	-	-	-	-	-
21	0.052	0.023	0.034	0.020	0.004
22	0.047	0.021	0.044	0.029	0.045
23	0.040	0.046	-0.007	0.012	0.014
24	0.033	0.039	-0.009	0.043	0.015
25	0.043	0.017	0.003	0.023	0.006
Average			0.024		
Std Deviation			0.016		

An experiment was conducted to compare the effects of buffer regulation to those without any control for a three-conveyor system in which objects directly transfer between conveyors and to determine a correlation between initial conditions and delivery output. The initial spacing and tracking error were recorded for all iterations. The results are tabulated in Tables A-5 through A-8.

Table A- 5: Initial Spacing and Tracking Error for Control Test of Three-Conveyor System

	Initial Spacing (in)				$\mathbf{e_j}$ (in)				
Test #	**j=2**	**3**	**4**	**5**	**1**	**2**	**3**	**4**	**5**
1	10.50	10.31	10.44	10.44	-0.39	-3.24	-3.88	-4.01	-5.39
2	10.50	10.31	10.44	10.44	-1.03	-0.12	0.51	3.42	5.93
3	10.50	10.31	10.44	10.44	-0.61	-2.29	4.49	4.11	6.14
4	10.50	10.31	10.44	10.44	-0.39	6.69	8.30	8.49	10.16
5	10.50	10.31	10.44	10.44	-1.39	3.92	3.92	5.84	7.51
6	10.50	10.31	10.44	10.44	-0.39	-3.24	-3.88	-4.01	-5.39

Table A- 6: Initial Spacing and Spacing Deviation of Three-Conveyor System

	Initial Spacing (in)				$\mathbf{\Delta S_j + S}$ (in)			
Test #	**j=2**	**3**	**4**	**5**	**1**	**2**	**3**	**4**
1	10.50	10.31	10.44	10.44	17.30	21.79	18.62	19.23

2	10.50	10.31	10.44	10.44	17.66	21.14	17.66	18.85
3	10.50	10.31	10.44	10.44	17.41	21.76	18.57	19.13
4	8.00	8.13	8.50	8.75	12.56	18.19	15.85	16.08
5	9.00	9.00	9.00	9.00	14.57	18.30	15.91	17.06
6	12.50	12.50	12.50	12.50	21.87	24.55	22.70	23.26
7	12.50	12.50	12.50	12.50	21.34	24.67	22.57	24.50
8	13.00	13.00	13.00	13.00	22.71	24.56	24.05	23.39
9	14.00	14.00	14.00	14.00	24.25	29.10	26.56	27.33
10	13.50	13.50	13.50	13.50	23.82	24.90	22.18	26.51
11	13.50	13.50	13.50	13.50	24.50	26.48	22.97	24.65

Table A- 7: Delivery Conditions of Three-Conveyor System without Singulator

	Landing Success					Tracking Error				
Test #	**j=1**	**2**	**3**	**4**	**5**	**1**	**2**	**3**	**4**	**5**
1	y	y	y	y	y	0.14	0.53	-0.08	0.49	-0.10
2	y	y	y	y	y	0.87	1.50	0.68	1.41	0.54
3	y	y	y	y	y	0.16	1.27	0.18	0.38	-0.24
4	y	n	n	n	n	0.43	-7.71	-4.18	10.43	-
5	y	y	n	n	n	0.62	-1.25	-6.82	11.51	-
6	y	y	y	y	y	0.18	0.62	1.87	1.13	0.53
7	y	y	y	y	y	-0.29	0.59	0.31	0.45	0.73
8	y	y	y	y	y	-0.47	0.58	0.34	0.63	0.47
9	y	y	p	p	n	-0.26	0.00	3.12	4.16	13.01
10	y	y	y	y	y	-	-	-	-	-
11	y	y	n	y	y	0.30	1.30	5.61	2.57	2.35

Table A- 8: Initial Spacing and Tracking Error for Additional Tests of Three-Conveyor System without Singulator

	Initial Spacing (in)				Tracking Error (in)				
Test #	**j=2**	**3**	**4**	**5**	**1**	**2**	**3**	**4**	**5**
1	10.50	10.31	10.44	10.44	0.0	1.0	0.4	0.5	0.5
2	10.50	10.31	10.44	10.44	0.0	0.0	-0.1	0.5	0.5
3	10.50	10.31	10.44	10.44	0.0	0.0	0.1	0.6	-0.1
4	10.50	10.31	10.44	10.44	0.1	0.0	-0.1	0.0	0.0
5	10.50	10.31	10.44	10.44	-0.1	0.6	0.0	-0.1	-0.1
6	10.50	10.31	10.44	10.44	-0.1	-0.1	0.6	-0.1	0.0
7	10.50	10.31	10.44	10.44	0.0	0.1	0.5	0.0	0.0
8	10.50	10.31	10.44	10.44	0.1	0.6	0.0	0.0	0.0
9	10.50	10.31	10.44	10.44	0.0	0.6	0.1	-0.1	0.1
10	10.50	10.31	10.44	10.44	0.0	0.0	-0.9	0.0	-0.1
11	9.50	9.50	9.50	9.50	0.0	-0.1	0.1	-0.4	-1.0
12	9.60	9.60	9.60	9.60	-0.1	-0.1	0.0	0.1	-0.1
13	9.70	9.70	9.70	9.70	-0.1	0.0	0.4	-0.1	-0.1
14	9.80	9.80	9.80	9.80	0.0	0.4	0.6	0.5	0.9
15	9.90	9.90	9.90	9.90	-0.1	0.1	0.5	-0.1	1.1
16	10.00	10.00	10.00	10.00	-0.1	0.1	-0.1	-0.6	0.5

17	10.10	10.10	10.10	10.10	0.0	0.0	-1.0	0.0	0.4
18	10.20	10.20	10.20	10.20	-0.1	0.1	0.1	0.1	0.9
19	10.30	10.30	10.30	10.30	-0.1	0.0	0.1	0.5	0.4
20	10.40	10.40	10.40	10.40	-0.1	0.1	0.0	0.4	0.5
21	11.38	11.93	10.68	11.85	-0.1	0.4	0.0	0.5	0.4
22	12.43	10.34	11.82	10.54	-0.1	0.1	-0.5	0.0	0.6
23	12.07	10.99	12.00	10.32	0.0	0.1	-0.5	0.1	0.6
24	11.06	11.82	10.45	11.25	0.1	0.0	0.1	0.0	0.6
25	10.27	11.50	11.88	11.71	0.1	0.1	-0.1	0.0	1.0
26	10.88	11.03	11.02	10.46	0.0	0.6	-0.4	0.5	1.4
27	10.79	10.89	11.39	10.31	0.1	0.1	-0.1	0.6	0.5
28	10.58	10.92	10.51	11.05	0.0	0.1	0.1	0.5	0.4
29	10.06	11.90	10.71	11.45	0.1	-0.1	0.0	0.0	1.0
30	10.54	10.36	11.33	10.55	-0.6	0.4	0.0	-0.1	0.0
31	11.54	12.17	10.54	10.35	0.0	-0.1	0.0	0.1	0.0
32	10.96	10.33	10.82	11.57	0.1	0.5	-0.4	0.0	0.0
33	12.26	10.70	10.64	11.49	0.0	0.1	-0.4	0.0	0.1
34	12.25	10.63	11.37	10.92	0.1	0.1	0.1	0.0	-0.1
35	12.06	11.15	10.50	10.52	0.1	-0.1	0.1	0.0	0.0

The tracking error data was not recorded for Iteration #10 of Table A- 7. For Iterations #4 and #5, e_5 was so large that it was not captured by the camera. In that table, "y" indicates a successful delivery, "p" indicates a partial delivery failure and "n" indicates a complete delivery failure.

APPENDIX B

EXPERIMENTAL RESULTS OF PRACTICAL IMPLEMENTATION OF BUFFER REGULATION

An experiment was conducted to test the modified position detection routine for irregular objects. The beamswitch was configured using both one and two columns of sensors to detect a model bird with a variable neck angle. The spacing and length measurement errors were recorded for both configurations, with results tabulated in Tables B-1 and B-2.

Table B- 1: Spacing Measurement Errors of Model Bird

	One Column (in)					Two Columns (in)				
I	**0°**	**30°**	**45°**	**60°**	**90°**	**0°**	**30°**	**45°**	**60°**	**90°**
1	0.256	0.140	0.268	0.237	0.240	0.106	0.061	0.185	0.232	0.338
2	0.183	0.044	0.265	0.298	0.211	0.179	0.121	0.165	0.223	0.211
3	0.182	0.135	0.214	0.168	0.219	0.152	0.147	0.211	0.226	0.242
4	0.225	0.144	0.267	0.232	0.305	0.170	0.098	0.186	0.252	0.278
5	0.240	0.158	0.235	0.217	0.263	0.217	0.162	0.214	0.217	0.343
6	0.273	0.129	0.238	0.228	0.244	0.182	0.179	0.236	0.214	0.314
7	0.203	0.087	0.249	0.258	0.317	0.185	0.076	0.224	0.217	0.296
8	0.188	0.108	0.271	0.222	0.260	0.188	0.146	0.177	0.174	0.320
9	0.223	0.106	0.230	0.161	0.226	0.199	0.047	0.177	0.244	0.337
10	0.205	0.108	0.235	0.199	0.229	0.196	0.141	0.167	0.287	0.327
11	0.200	0.114	0.252	0.276	0.223	0.103	0.157	0.190	0.260	0.287
12	0.265	0.112	0.243	0.205	0.296	0.165	0.140	0.157	0.227	0.370
13	0.263	0.153	0.237	0.379	0.246	0.140	0.134	0.260	0.274	0.334
14	0.214	0.100	0.284	0.230	0.273	0.209	0.102	0.227	0.229	0.328
15	0.258	0.108	0.258	0.287	0.247	0.240	0.161	0.191	0.199	0.323
Avg	0.225	0.116	0.250	0.240	0.253	0.175	0.125	0.198	0.232	0.310
Std	0.032	0.029	0.019	0.055	0.032	0.038	0.040	0.030	0.029	0.041

Table B- 2: Length Measurement Errors of Model Bird

	One Column (in)					Two Columns (in)				
i	**0°**	**30°**	**0°**	**30°**	**0°**	**30°**	**0°**	**30°**	**0°**	**30°**
1	0.540	0.254	0.430	0.473	0.491	0.894	0.685	0.767	0.897	0.845
2	0.500	0.245	0.470	0.446	0.512	0.921	0.679	0.733	0.906	0.891
3	0.485	0.260	0.455	0.470	0.460	0.888	0.645	0.737	0.912	0.855
4	0.485	0.227	0.458	0.485	0.455	0.840	0.694	0.761	0.940	0.855
5	0.494	0.282	0.454	0.488	0.460	0.873	0.691	0.757	0.848	0.885
6	0.479	0.300	0.428	0.497	0.454	0.867	0.658	0.718	0.873	0.855
7	0.473	0.294	0.482	0.503	0.510	0.827	0.682	0.731	0.927	0.888
8	0.488	0.315	0.406	0.442	0.482	0.918	0.600	0.779	0.870	0.846
9	0.461	0.254	0.439	0.473	0.488	0.855	0.648	0.736	0.888	0.840
10	0.503	0.294	0.433	0.515	0.455	0.858	0.691	0.706	0.842	0.921
11	0.518	0.224	0.439	0.470	0.470	0.855	0.642	0.749	0.842	0.861
12	0.473	0.288	0.430	0.473	0.473	0.925	0.664	0.743	0.919	0.867
13	0.494	0.297	0.467	0.366	0.479	0.846	0.667	0.706	0.885	0.900
14	0.458	0.230	0.482	0.491	0.512	0.864	0.637	0.739	0.876	0.873
15	0.470	0.303	0.444	0.430	0.485	0.852	0.694	0.788	0.870	0.910
Avg	0.488	0.271	0.448	0.468	0.479	0.872	0.665	0.743	0.886	0.873
Std	0.022	0.030	0.021	0.036	0.021	0.031	0.027	0.024	0.030	0.025

An experiment was conducted to investigate the effects of additional spacing variability on the performance of the buffer regulation algorithm implemented on a three-conveyor system. A transfer mechanism bridging the gap between the 1st and 2nd conveyors imparted a random time delay upon objects transitioning between conveyors. The initial spacing, spacing deviation, delivery condition and tracking error were recorded for all iterations. The results are tabulated in Tables B-3 and B-4.

Table B- 3: Initial Spacing and Spacing Deviation of Three-Conveyor System with Singulator

	Initial Spacing (in)				$\Delta S_j + S$ (in)			
Test #	**j=2**	**3**	**4**	**5**	**2**	**3**	**4**	**5**
1	10.50	10.31	10.44	10.44	18.73	26.06	20.15	23.56
2	10.50	10.31	10.44	10.44	27.69	25.22	19.26	26.91
3	10.50	10.31	10.44	10.44	18.82	26.83	19.72	23.20
4	10.50	10.31	10.44	10.44	19.21	24.33	21.11	27.83
5	10.50	10.31	10.44	10.44	24.45	22.45	24.72	26.38
6	7.50	7.50	7.00	6.75	13.90	32.12	10.92	19.18
7	7.00	7.50	7.50	7.00	15.21	26.89	16.12	21.78
8	7.50	8.00	1.00	1.00	20.00	27.42	11.70	22.18
9	9.00	8.50	8.00	8.50	24.65	22.97	15.08	23.60

10	9.00	8.50	8.50	9.00	23.77	23.28	18.45	24.17
11	8.50	8.50	8.00	8.50	27.36	18.81	17.63	23.82
12	9.50	9.50	9.50	9.50	23.03	26.95	26.49	17.35
13	9.50	9.50	9.50	9.50	21.59	25.49	25.00	23.18
14	13.50	13.50	13.50	13.50	25.20	25.27	22.28	30.37
15	13.50	13.50	13.50	13.50	28.62	24.13	25.22	24.09
16	13.50	13.50	13.50	13.50	17.18	22.09	18.56	20.52

Table B- 4: Delivery Conditions of Three-Conveyor System with Singulator

	Landing Success					Tracking Error				
Test #	**j=1**	**2**	**3**	**4**	**5**	**1**	**2**	**3**	**4**	**5**
1	y	y	n	p	y	-1.52	-0.68	6.39	1.84	0.20
2	y	y	n	y	n	-1.23	1.86	6.98	1.13	11.94
3	y	y	n	p	y	-0.21	0.53	6.87	3.46	0.72
4	y	y	y	y	y	-0.73	-0.96	0.34	-1.18	0.83
5	y	y	y	y	y	-0.48	-0.75	0.74	-0.40	-0.10
6	y	n	p	p	p	0.75	-5.92	5.09	-4.59	-3.27
7	p	p	y	p	p	2.57	-3.61	1.27	-3.57	-3.87
8	p	y	n	n	p	3.14	0.68	13.07	6.00	3.56
9	y	y	y	p	p	-0.47	-0.67	0.25	-3.19	-3.69
10	y	y	y	y	y	-1.11	-1.84	-1.04	-0.80	-1.82
11	y	n	n	p	y	-0.67	8.51	9.40	2.35	1.19
12	y	y	y	n	y	-0.84	-1.27	0.23	8.93	1.80
13	y	y	y	p	y	-0.57	-0.13	0.69	3.17	-0.57
14	y	y	y	y	y	-1.94	-1.06	1.62	-0.15	4.02
15	y	n	n	n	n	-1.62	4.08	5.24	5.09	12.95
16	y	p	p	p	n	-1.32	2.98	2.58	2.34	13.58

REFERENCES

Banner Engineering "A-GAGE™ High-Resolution MINI-ARRAY™ Instruction Manual," P/N 64118 rev. A, 2005

Berry, "Poultry Harvester" US Patent #5,361,727, November 8, 1994

Copley Controls Corp., "Xenus™ User Guide," P/N 95-00286-000, Version 2.0, 2005

Cramer, "Apparatus and process for cutting chicken," USPTO #3,943,600, 1976

Dumont, G. and Huzmezan, M., "Concepts, Methods and Techniques in Adaptive Control," Transactions on Control Systems Technology Proceedings of ACC 2002, Anchorage, USA

Hiyama, T., Ueno, D., Yamashiro, S., Yamagishi, M., Shimizu, M., "Fuzzy logic switching control for electrical double-layer energy capacitor system for stability enhancement", Power Engineering Society Summer Meeting, 2000. IEEE Volume 4

Inoue T. and Nakano M., "High accuracy control of a proton synchrotron magnet power supply," in IFAC Conf. Rec., 1981, pp. 216–221. http://www-ics.acs.i.kyoto-u.ac.jp/~yy/Papers/RepetitiveControldocfin.pdf#search=%22repetitive%20control%22

Joni, J., "Quasi-Static Force Analysis of an Automated Live-Bird Transfer System," Master's Thesis, 2000, pp. 63-71.

Kuo, B., Automatic Control Systems, 7th ed., Prentice Hall, 1995

Lan, C.-C. and K.-M. Lee, "An Analytical Contact Model for Design of Compliant Fingers," *Proc. of the 2006 International Symposium on Flexible Automation (ISFA)*, Osaka, Japan, July 10-12, 2006, pp 905-911.

Lauzon, S., Ma, A., Mills, J. and Benhabib, B., "Application of Discrete-Event-System Theory to Flexible Manufacturing," IEEE Control Systems, 1996

Lee, K.-M., "Intelligent Automated Transfer of Live Broilers to Shackle Line," Project Report P3200-140. Georgia Agriculture Technology Research Program, July 1, 1998.

Lee, K.-M. Gogate, R. and Carey, Richard, "Automated Singulating System for Transfer of Live Broilers," *Proceedings of the 1998 IEEE International Conference on Robotics and Automation*, May 16-21, Leuven, Belgium.

Lee, K-M., J. Joni, and X. Yin, "Compliant Grasping Force Modeling for Handling of Live Objects," *Proceedings of the IEEE ICRA2000,* May 21-26, Seoul, Korea, pp. 1059-1064.

Lee, K.-M., "Design Criteria for Developing an Automated Live-Bird Transfer System," IEEE TRANSACTIONS ON ROBOTICS AND AUTOMATION, VOL. 17, NO. 4, AUGUST 2001

Li, Q. and K.-M. Lee, "Effects of Color Characterization on Computational Efficiency of Feature Detection with Live-object Handling Applications," *Proc. of IEEE/ASME AIM2005*, July 24-28, 2005, Monterey, California, pp. 225-230.

Lin, F., "Robust and Adaptive Supervisory Control of Discrete Event Systems," IEEE TRANSACTIONS ON AUTOMATIC CONTROL VOL. 38, NO. 12, DECEMBER, 1993

OSHA, http://stats.bls.gov/iif/oshwc/osh/os/ostb1487.txt

Peterson, J., "Petri Nets," Computing Surveys, Vol 9, No. 3, September, 1977

Porter, B., "Are bang-bang minimum-time control policies evolutionarily inevitable?", IEEE International Conference on Systems, Man, and Cybernetics, 1996., Volume 3, 14-17 Oct. 1996 pg: 2422 - 2427 vol.3

Ramadge, P. and Wonham W., "The Control of Discrete Event Systems" PROCEEDINGS OF THE IEEE, VOL 77, NO 1, JANUARY 1989

Trio Motion Technology "Motion Coordinator Technical Reference Manual," Sixth Edition, Revision 5, 2005

Tomizuka, M., "Zero Phase Error Tracking Algorithm for Digital Control," Journal of Dynamic Systems, Measurement, and Control, March 1987, Vol.109

Toshiba, "G7 Adjustable Speed Drive Operation Manual,"D/N 51546-009, March, 2005

Uzam, M. and Jones, A., "Discrete Event Control System Design Using Automation Petri Nets and their Ladder Diagram Implementation" International Journal of Advanced Manufacturing Technology, 1998

http://www.poultry.org/labor_frontline.htm

Yin, X., K.-M. Lee, and C.-C. Lan, "Computational Models For Predicting The Deflected Shape Of A Non-Uniform, Flexible Finger," *Proc. of the IEEE ICRA2004*, New Orleans, LA., 26 April - 1 May, vol. 3, pp. 2963- 2968.